This is to certify that the

thesis entitled

RESPONSE OF SIMPLE BEAM TO
SPATIALLY VARYING SEISMIC EXCITATION

presented by

WEIJUN WANG

has been accepted towards fulfillment
of the requirements for

M.S degree in CE

Major professor

Date February 4, 1988

RESPONSE OF SIMPLE BEAM TO SPATIALLY VARYING SEISMIC EXCITATION

by

Weijun Wang

A THESIS

Submitted to

Michigan State University

in partial fulfillment of the requirements

for the degree of

MASTER OF SCIENCE

Department of Civil and Environmental Engineering

1988

ABSTRACT

RESPONSE OF SIMPLE BEAM TO
SPATIALLY VARYING SEISMIC EXCITATION

By

Weijun Wang

The stochastic response of a simply supported beam is analyzed by using a space-time earthquake ground motion model. The effect of the spatial variation of ground motion is considered and results for several types of support motion correlations are compared. For practical use, an approximate method which can be used to quickly estimate the beam response is proposed.

ACKNOWLEDGEMENTS

The research described in this report was supported by the National Science Foundation under Grant No. ECE 8605184 and a grant from the Division of Engineering Research, Michigan State University. The author is grateful for this support.

The author wishes to thank Professor R. Harichandran for his continuous encouragement and direction during this work. The author is also grateful to Professors R. Wen and T. Wolff for reviewing the manuscript and suggesting improvements.

TABLE OF CONTENTS

LIST OF FIGURES

LIST OF SYMBOLS

The following symbols are used in this paper:

c - damping per unit length;

EI - flexural rigidity of beam;

f - linear frequency (Hz);

f_g - fundamental linear frequency of soil;

f_j - modal linear frequency;

f_p - frequency at which the Kanai-Tajimi spectrum has its peak;

$f(t)$ - load which is the function of time;

$H_j(\omega)$ - modal frequency response function;

$H_{y_j}(\omega,x)$ - modal displacement frequency response function;

$H_{u_d}(\omega,x,\xi)$ - frequency response function (transfer function);

$Y_j(x)$ - modal displacement;

L - length of beam;

m - mass per unit length;

$R_{\ddot{u}_A}(\tau)$, $R_{\ddot{u}_B}(\tau)$ - autocorrelation functions of accelerations at A and B;

$R_{\ddot{u}_A\ddot{u}_B}(\tau)$ - cross correlation function of accelerations at A and B;

S_o - constant intensity parameter;

$S_{\ddot{u}_g}(w)$ - spectral density function of ground acceleration;

$S_{\ddot{u}_A\ddot{u}_B}(w)$ - cross spectral density of accelerations at A and B;

$u(x,t)$ - horizontal transverse displacement of beam;

$\ddot{u}_A(t)$, $\ddot{u}_B(t)$ - accelerations at supports A and B of beam;

$u_s(x,t)$ - pseudo-static displacement;

$u_d(x,t)$ - dynamic displacement;

x - length along beam;

V - apparent seismic wave propagation velocity from A to B;

β_g - ratio of critical damping of soil;

$\delta(x,\xi)$ - Dirac delta function;

$\psi_j(x)$ - mode shape;

ζ_j - modal damping ratio;

$\Phi_{jk}(\omega)$ - modal response cross spectral density function;

ν - separation distance;

$\rho(\nu,f)$ - frequency-dependent spatial correlation function;

$\sigma_i^2(x)$ - variance of curvature response for case i;

$\sigma_{u_d}^2(x)$ - variance of dynamic displacement response;

$\sigma_{u''}^2(x)$ - variance of curvature response;

ΔA - area corresponding to correction $\Delta\sigma^2(x)$;

$\Delta\sigma^2(x)$ - correction to approximation of $\sigma_{u''}^2(x)$;

ω - circular frequency (rad/sec);

ω_g - fundamental circular frequency of soil;

ω_j - modal circular frequency;

Superscripts

$\cdot$ - first partial derivative with respect to time;

$\ddot{}$ - second partial derivative with respect to time;

$''$ - second partial derivative with respect to x;

iv - fourth partial derivative with respect to x.

1. INTRODUCTION

Due to the complexity of the earth's structure (inhomogeneity, anisotropy, etc.), rigorous investigations of structural responses to earthquake ground motions should consider the effects of wave propagation and spatial correlation of ground motions. These effects would be expected to be especially significant for large structures such as bridges, lifelines, dams, etc. Studies of the space-time variation of strong ground motion and its effect on structures has only recently gained prominence (Loh, et al., 1982; Bolt, et al., 1984; Harichandran & Vanmarcke, 1986; Harichandran, 1987).

In this report, the simplest model of a bridge or lifeline - a simply supported beam - is studied, and attention is focused on the stochastic response under seismic support excitations. Consideration is given to both wave propagation effects and spatial correlation effects. A stochastic space-time ground motion model resulting from studies of the space-time variation of earthquake ground motion based on the data obtained from the SMART-1 seismograph array in Lotung, Taiwan (Harichandran & Vanmarcke 1986) is used to analyze the effect of spatial variation of ground motion on structural responses.

The bending response of the beam due to transverse base-excitation is analyzed. In the analysis, stationary random vibration is assumed. The maximum response of the structure for various types of support motions with different characteristic parameters are compared. Also,

the variations of the maximum response with variations of the natural frequency and length of beam as well as the fundamental frequency and damping of the soil are determined. Finally, approximate methods for the quick evaluation of the beam responses are evaluated.

2. ANALYSIS OF SIMPLY SUPPORTED BEAM

2.1 Ground Motion Model

In order to study the response of structures to spatially varying earthquake ground motion, a suitable ground motion model is required. In this study a space-time ground motion model proposed by Harichandran and Vanmarcke (1986) is used. In this model the ground accelerations are assumed to constitute a homogeneous random field. The point spectral density function (SDF) of the ground acceleration, $S_{\ddot{u}_g}(\omega)$, is therefore assumed to be the same at all spatial locations. The correlation between the accelerations at two different points is characterized by a coherency function $\rho(\nu,f)$, and the phase due to the time delay caused by wave propagation is accounted for by an exponential function, $\exp(-i\omega\nu/V)$. The cross SDF between the accelerations at two locations A and B is then written as the product of the point SDF, coherency function and phase delay

$$S_{\ddot{u}_A\ddot{u}_B}(\omega) = S_{\ddot{u}_g}(\omega)\ \rho(\nu,f)\ e^{-i\omega\nu/V} \qquad (2\text{-}1)$$

where

$$\rho(\nu,f) = A \exp\left[-\frac{2\nu}{\alpha\theta(f)}(1 - A + \alpha A)\right] + (1 - A)\exp\left[-\frac{2\nu}{\theta(f)}(1 - A + \alpha A)\right] \qquad (2\text{-}2)$$

$$\theta(f) = k\left[1 - (f/f_o)^b\right]^{-1/2} \qquad (2\text{-}3)$$

A, α, k, f_o and b are empirical constants, whose values for the radial components of a specific earthquake in Taiwan (Event 20 recorded by the SMART-1 array) were:

$$A = 0.736;\ \alpha = 0.147;\ k = 5{,}210;\ f_o = 1.09 \text{ and } b = 2.78; \qquad (2\text{-}4)$$

$f = \omega/2\pi$ = linear frequency;

ν = separation between locations A and B = L for the simply supported beam;

V = apparent wave propagation velocity in direction AB.

Any reasonable model may be used for the point SDF, and for a single-span beam the Kanai-Tajimi spectrum is adequate. This spectrum is obtained by passing a white-noise bedrock acceleration, whose spectrum is S_o, through a filter (transfer function) corresponding to a one degree-of-freedom dynamic system, and has the form

$$S_{\ddot{u}_g}(\omega) = \left[\frac{(1 + 4\beta_g^2[\omega/\omega_g]^2)}{(1 - [\omega/\omega_g]^2)^2 + 4\beta_g^2[\omega/\omega_g]^2}\right] S_o \qquad (2\text{-}5)$$

where ω_g and β_g are the fundamental frequency and damping of the ground, respectively, and S_o is an intensity parameter. The parameters ω_g and β_g are usually estimated by fitting equation (2-5) to the spectra of real acceleration records.

2.2 Random Vibration Analysis of Response

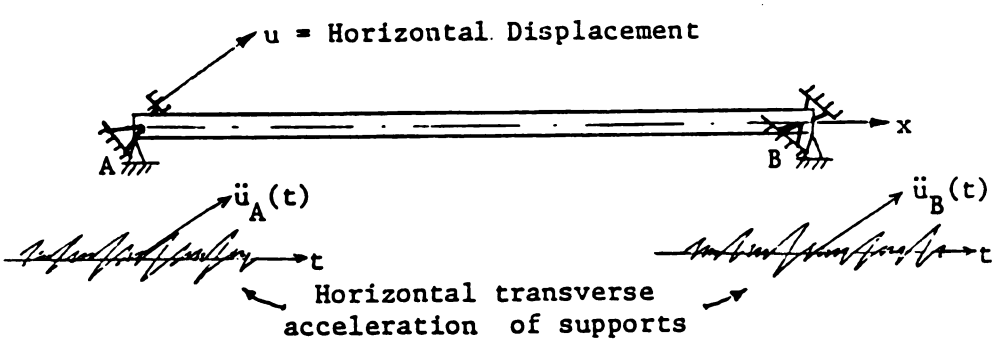

Figure 2-1 : Simple Beam With Support Excitation

Consider a simply supported beam excited by horizontal transverse accelerations, $\ddot{u}_A(t)$ and $\ddot{u}_B(t)$, at supports A and B, respectively, as shown in Figure 2-1 above. For a constant flexural rigidity EI, mass, m, per unit length and coefficient of viscous damping, c, per unit length, the equation of motion for the beam is

$$m \frac{\partial^2 u}{\partial t^2} + c \frac{\partial u}{\partial t} + EI \frac{\partial^4 u}{\partial x^2} = 0 \qquad (2\text{-}6)$$

where u is the horizontal transverse displacement of the beam.

Decomposing the displacement into a pseudo-static part, u_s, and a dynamic part, u_d, we obtain:

$$u(x,t) = u_s(x,t) + u_d(x,t) \qquad (2\text{-}7)$$

where $u_s(x,t) = u_A(t) + [u_B(t) - u_A(t)]\, x/L$

x = distance from support A;

L = length of the beam.

Substituting (2-7) into (2-6)

$$m\ddot{u}_d + c\dot{u}_d + EI\, u_d^{iv} = - m\ddot{u}_s - c\dot{u}_s \qquad (2\text{-}8)$$

For light damping $c\dot{u}_s$ is small compared to $m\ddot{u}_s$, and the equation of motion can be written as

$$\ddot{u}_d + \frac{c}{m}\dot{u}_d + \frac{EI}{m} u_d^{iv} = g(x,t) \qquad (2\text{-}9)$$

where

$$g(x,t) \approx - m\ddot{u}_s = - \ddot{u}_A\left(1 - \frac{x}{L}\right) - \ddot{u}_B \frac{x}{L} \qquad (2\text{-}10)$$

and the boundary conditions are $u_d(0,t) = u_d(L,t) = 0$.

Using modal synthesis, we let

$$u_d(x,t) = \sum_j \psi_j(x) Y_j(t) \qquad (2\text{-}11)$$

It is well known that for a simply supported beam with length L, the normalized mode shape , $\psi_j(x)$, is

$$\psi_j(x) = \left[\frac{2}{L}\right]^{\frac{1}{2}} \sin \frac{j\pi x}{L} \tag{2-12}$$

and the natural frequency ω_j is

$$\omega_j = \left(\frac{EI}{m}\right)^{\frac{1}{2}} \left(j\frac{\pi}{L}\right)^2 \tag{2-13}$$

Now consider a point load at $x = \xi$: $g(x,t) = \delta(x-\xi)f(t)$. Substituting (2-11), (2-12) and (2-13) into (2-9), mutiplying by ψ_k and integrating with respect to x over the length of beam, we obtain

$$\ddot{Y}_j + \frac{c}{m}\dot{Y}_i + \omega_j^2 Y_j = \frac{\int_0^L \psi_j(x)\, f(t)\, \delta(x-\xi)\, dx}{L}$$

$$= \psi_j(\xi)\, f(t) \tag{2-14}$$

since

$$\int_0^L \psi_j \psi_k \, dx = 0 \qquad j \neq k$$

and

$$\int_0^L \psi_j \psi_k \, dx = L \qquad j = k$$

for the harmonic input $f(t) = e^{i\omega t}$, the response is

$$Y_j(\omega;\xi) = H_{y_j}(\omega;\xi)\, e^{i\omega t} \tag{2-15}$$

Substituting (2-15) into (2-14), we obtain

$$H_{y_j}(\omega;\xi) = \left[\frac{1}{\omega_j^2 - \omega^2 + i\omega\frac{c}{m}}\right] \psi_j(\xi)$$

$$= H_j(\omega)\, \psi_j(\xi) \tag{2-16}$$

where $$H_j(\omega) = \frac{1}{\omega_j^2 - \omega^2 + i\omega\frac{c}{m}}$$

In $H_j(\omega)$, $\frac{c}{m}$ is the modal bandwidth and is constant. Therefore, the ratio of critical damping for mode j, $\zeta_j = \frac{c}{2m\omega_j}$, varies inversely with natural frequency, and we can rewrite

$$H_j(\omega) = \frac{1}{\omega_j^2 - \omega^2 + i2\zeta_j\omega_j\omega} \tag{2-17}$$

Using (2-15) and (2-16), equation (2-11) becomes

$$u_d(x,t;\xi) = \sum_j \psi_j(x)\, Y_i(t;\xi)$$

$$= \sum_j \psi_j(x)\, H_j(\omega)\, \psi_j(\xi)\, f(t)$$

or

$$u_d(x,t;\xi) = H_{u_d}(x,\omega;\xi)\, f(t) \tag{2-18}$$

where

$$H_{u_d}(x,\omega;\xi) = \sum_j \psi_j(x)\, H_j(\omega)\, \psi_j(\xi)$$

is the frequency response function (or transfer function).

For stationary support excitations, the autocorrelation function, $R_g(x_1,x_2,\tau)$, of the input $g(x,t)$ is

$$R_g(x_1,x_2,\tau) = E\,[g(x_1,t)\, g(x_2,t+\tau)]$$

$$= \left[1 - \frac{x_1}{L}\right]\left[1 - \frac{x_2}{L}\right] R_{\ddot{u}_A}(\tau) + \frac{x_1x_2}{L^2} R_{\ddot{u}_B}(\tau)$$

$$+ \left[1 - \frac{x_1}{L}\right]\frac{x_2}{L} R_{\ddot{u}_A\ddot{u}_B}(\tau) + \frac{x_1}{L}\left[1 - \frac{x_2}{L}\right] R_{\ddot{u}_B\ddot{u}_A}(\tau) \tag{2-19}$$

where $R_{\ddot{u}_A}(\tau)$ and $R_{\ddot{u}_B}(\tau)$ are the autocorrelation functions of $\ddot{u}_A$ and $\ddot{u}_B$, respectively, and $R_{\ddot{u}_A\ddot{u}_B}(\tau)$ and $R_{\ddot{u}_B\ddot{u}_A}(\tau)$ are the cross correlation functions of $\ddot{u}_A$ and $\ddot{u}_B$. (Note that $R_{\ddot{u}_A\ddot{u}_B}(\tau) = R_{\ddot{u}_A\ddot{u}_B}(-\tau)$.)

Taking the Fourier transform of $R_g(x_1,x_2,\tau)$, we can obtain the spectral density function of $g(x,t)$

$$S_g(x_1,x_2,\omega) = \left[1 - \frac{x_1}{L}\right]\left[1 - \frac{x_2}{L}\right] S_{\ddot{u}_A}(\omega) + \frac{x_1x_2}{L^2} S_{\ddot{u}_B}(\omega)$$

$$+ \left[1 - \frac{x_1}{L}\right]\frac{x_2}{L} S_{\ddot{u}_A\ddot{u}_B}(\omega) + \frac{x_1}{L}\left[1 - \frac{x_2}{L}\right] S_{\ddot{u}_B\ddot{u}_A}(\omega) \tag{2-20}$$

where $S_{\ddot{u}_A}(\omega)$ and $S_{\ddot{u}_B}(\omega)$ are the autospectra of $\ddot{u}_A$ and $\ddot{u}_B$, respectively, and $S_{\ddot{u}_A\ddot{u}_B}(\omega)$ and $S_{\ddot{u}_B\ddot{u}_A}(\omega)$ are the cross-spectra of $\ddot{u}_A$ and $\ddot{u}_B$.

The spectral density function of the response is (Crandall, 1979)

$$S_{u_d}(x_1,x_2,\omega) = \int_0^L \int_0^L H_{u_d}(x_1,-\omega;\xi_1)\, H_{u_d}(x_2,-\omega;\xi_2)\, S_g(\xi_1,\xi_2,\omega)\, d\xi_1\, d\xi_2$$

$$= \sum_{j=1}^{\infty} \sum_{k=1}^{\infty} \psi_j(x_1)\, \psi_k(x_2)\, H_j(-\omega)\, H_k(\omega)\, \Phi_{jk}(\omega) \qquad (2\text{-}21)$$

where $\Phi_{jk}(\omega)$, the modal response cross spectral density function, is

$$\Phi_{jk}(\omega) = \int_0^L \int_0^L \psi_j(\xi_1)\, \psi_k(\xi_2)\, S_g(\xi_1,\xi_2,\omega)\, d\xi_1\, d\xi_2 \qquad (2\text{-}22)$$

According to the definition the variance of response is the value of autocorrelation function $R_g(x_1,x_2,\tau)$ when $x_1 = x_2$ and $\tau = 0$. Since the spectral density function $S_g(x_1,x_2,\omega)$ and autocorrelation function $R_g(x_1,x_2,\tau)$ are Fourier transform pair and the spectral density function gives a decomposition of the variance (power) with frequency, so the variance of the dynamic displacement at any locations along the beam is the integration of spectral density function at the all frequency range with $x_1 = x_2 = x$

$$\sigma^2_{u_d}(x) = \int_{-\infty}^{\infty} S_{u_d}(x,x,\omega)\, d\omega$$

$$= \sum_{j=1}^{\infty} \sum_{k=1}^{\infty} \psi_j(x)\, \psi_k(x) \int_{-\infty}^{\infty} H_j(-\omega)\, H_k(\omega)\, \Phi_{jk}(\omega)\, d\omega \qquad (2\text{-}23)$$

For well-separated modes, the contributions from the cross-terms (for which $j \neq k$) are very small compared to the terms for which $j = k$. Thus, as an approximation, we can write

$$\sigma^2_{u_d}(x) \approx \sum_{j=1}^{\infty} [\psi_j(x)]^2 \int_{-\infty}^{\infty} |H_j(\omega)|^2 \Phi_{jj}(\omega)\, d\omega \qquad (2\text{-}24)$$

In order to evaluate $\Phi_{jj}(\omega)$, we use the ground motion model specified by equations (2-1) and (2-2). $\Phi_{jj}(\omega)$ can then be obtained in closed form as

$$\Phi_{jj}(\omega) = \frac{4L}{(j\pi)^2} [1 - (-1)^j \rho(L,f) \cos(\omega L/V)]\, S_{\ddot{u}_g}(\omega) \qquad (2\text{-}25)$$

In engineering design, we are often more interested in stress levels, and the stress due to bending is propotional to the curvature u" (the second derivative of displacement u with respect to distance x. For a simply supported single span beam

$$u'' = u''_d + u''_s = u''_d$$

or

$$u'' = \frac{\partial^2}{\partial x^2} u_d = \frac{\partial^2}{\partial x^2} \left[\sum_j \psi_j(x) Y_j(t)\right]$$

$$= \sum_j \frac{\partial^2}{\partial x^2} \psi_j(x)\, Y_j(t) = \sum_j \psi''_j(x)\, Y_j(t) \qquad (2\text{-}26)$$

Repeating the same procedure as before (the only difference being the use of $\psi''_j(x)$ instead of $\psi_j(x)$), the variance of the curvature is

$$\sigma^2_{u''}(x) = \sigma^2_{u''_d}(x) = \sum_{j=1}^{\infty} \sum_{k=1}^{\infty} \psi''_j(x)\, \psi''_k(x) \int_{-\infty}^{\infty} H_j(-\omega)\, H_k(\omega)\, \Phi_{jk}(\omega)\, d\omega$$

$$\approx \sum_{j=1}^{\infty} [\psi''_j(x)]^2 \int_{-\infty}^{\infty} |H_j(\omega)|^2 \Phi_{jj}(\omega)\, d\omega \qquad (2\text{-}27)$$

where

$$\psi''_j(x) = \frac{d^2}{dx^2} \psi_j(x) = -\left[\frac{2}{L}\right]^{1/2} \left[\frac{j\pi}{L}\right]^2 \sin \frac{j\pi x}{L} \qquad (2\text{-}28)$$

2.3 Numerical Results

2.3.1 General Excitation

Equation (2-27) represents the variance of curvature, $\sigma^2_{u''}$, for the general case, i.e., considering the correlation between different supports excitations as well as the phase shift (or the time delay for the seismic waves to travel from one location to another). If some parameters (such as the length L and fundamental frequency f_1 of the beam, the fundamental frequency f_g and damping β_g of the ground) change, $\sigma^2_{u''}(x)$ will also change. Some numerical results are presented here which investigate the effect of these parameters on the beam response. A computer program was written by the author to perform the necessary calculations. Due to the very small contribution of higher modes to $\sigma^2_{u''}(x)$, and the symmetry in $\sigma^2_{u''}(x)$ along the beam, only the first four modal responses were accounted for and only the left half of beam was examined.

Figure 2-2 depicts the distribution of the normalized variance of curvature, $\sigma^2_{u''}(x)$, along the beam. The normalization is performed by dividing the values of $\sigma^2_{u''}(x)$ by $\sigma^2_{u''}(L/2)$. It can be seen that $\sigma^2_{u''}(x) = 0$ at the supports (because the moment is zero) and the maximum value of $\sigma^2_{u''}(x)$ is at midlength. Since we are mostly interested in the maximum variance, we will mainly focus our attention on $\sigma^2_{u''}(x)$ at the midspan, i.e., at $x = L/2$.

It should be pointed out, however, that the maximum value of $\sigma^2_{u''}$ is not always at the midspan, and may appear at some other location for specific cases. Figure 2-3 shows an example of this. For the case of $f_g = 4$ Hz, $f_1 = 1$ Hz and $\beta_g = 0.35$, the maximum values of $\sigma^2_{u''}$ are at approximately $x = 0.4L$ and $x = 0.6L$. This occurs due to the fact that when fundamental frequency of the structure, f_1, is equal to 1 Hz, the

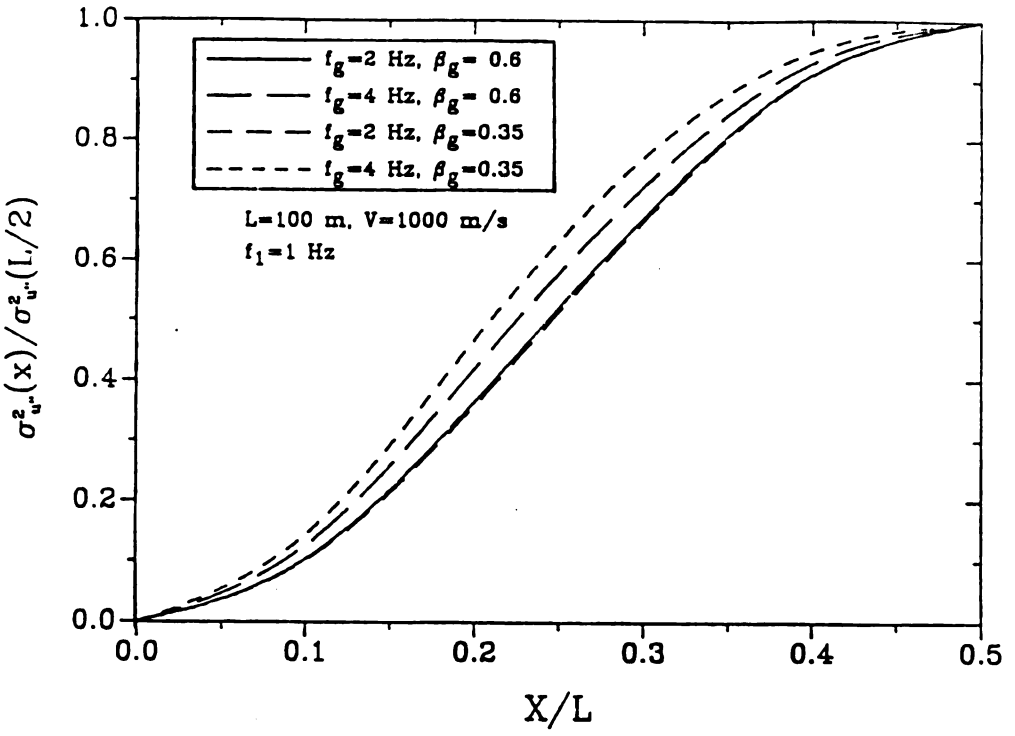

Figure 2-2 : Distribution of $\sigma^2_{u''}$ for Different β_g and f_g

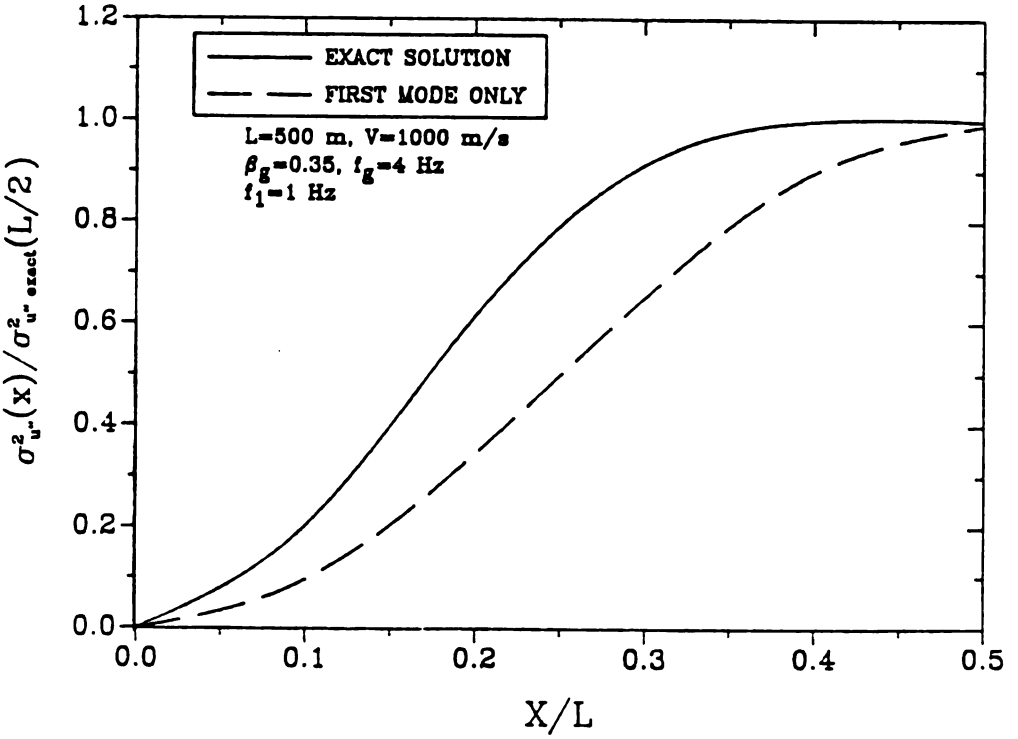

Figure 2-3 : $\sigma^2_{u''}$ for Exact Solution and First Mode Approximation

second mode frequency is 4 Hz and is equal to the ground motion frequency. Hence for this case the second mode response becomes significant, and the maximum values of $\sigma^2_{u''}$ for the second mode response are at x = L/4 and x = 3L/4. The combination of the first four modal responses makes the maximum values of $\sigma^2_{u''}$ shift slightly to the two points x = 0.4L and x = 0.6L. However, the difference between $\sigma^2_{u''}(L/2)$ and $\sigma^2_{u'',max}$ is small, usually less than 10%, and therefore this rare situation can perhaps be neglected.

Figures 2-4 to 2-7 show how the parameters f_1, L, β_g and f_g affect $\sigma^2_{u''}$. Figure 2-4 and 2-5 indicate that $\sigma^2_{u''}$ is very sensitive to changes in f_1 and L. As the natural frequency and length of the structure increase, $\sigma^2_{u''}$ decreases very rapidly. It should be noted, however, that the variance of the stress response is equal to $(EI)^2\sigma^2_{u''}$, and EI is expected to be quite different for beams of different fundamental frequencies and lengths. Figure 2-6 shows that $\sigma^2_{u''}$ does not change significantly with β_g over its normal range. When the damping ratio of the ground, β_g, decreases below that of the structure, $\zeta_1 = 0.05$, $\sigma^2_{u''}$ increases sharply, but when β_g is larger than ζ_1, $\sigma^2_{u''}$ decreases only slightly. (It should be noted that β_g is almost never less than ζ_1.) As expected, Figure 2-7 shows that the maximum value of $\sigma^2_{u''}$ occurs when the ground motion frequency, f_g, is near the fundamental natural frequency of the structure (resonance). When f_g tends to zero (i.e., when the base excitation becomes static) the dynamic curvature response vanishes, as it should. When f_g is higher than and well separated from the structure fundamental frequency, f_1, $\sigma^2_{u''}$ is approximately constant.

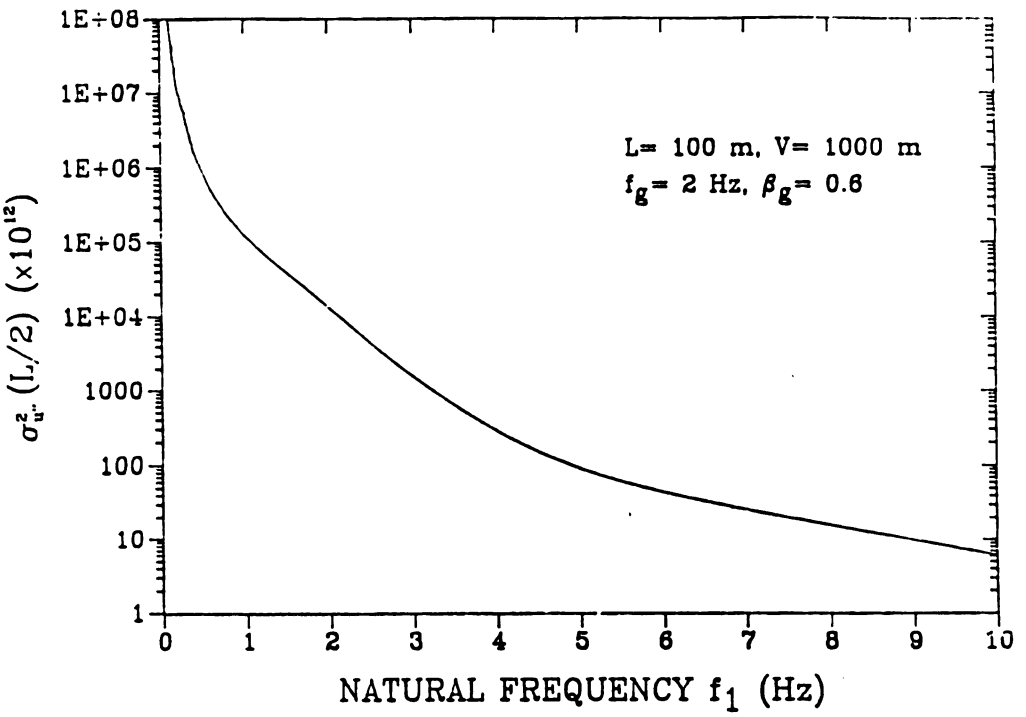

Figure 2-4 : Effect of Fundament Frequency of Beam on $\sigma^2_{u''}$

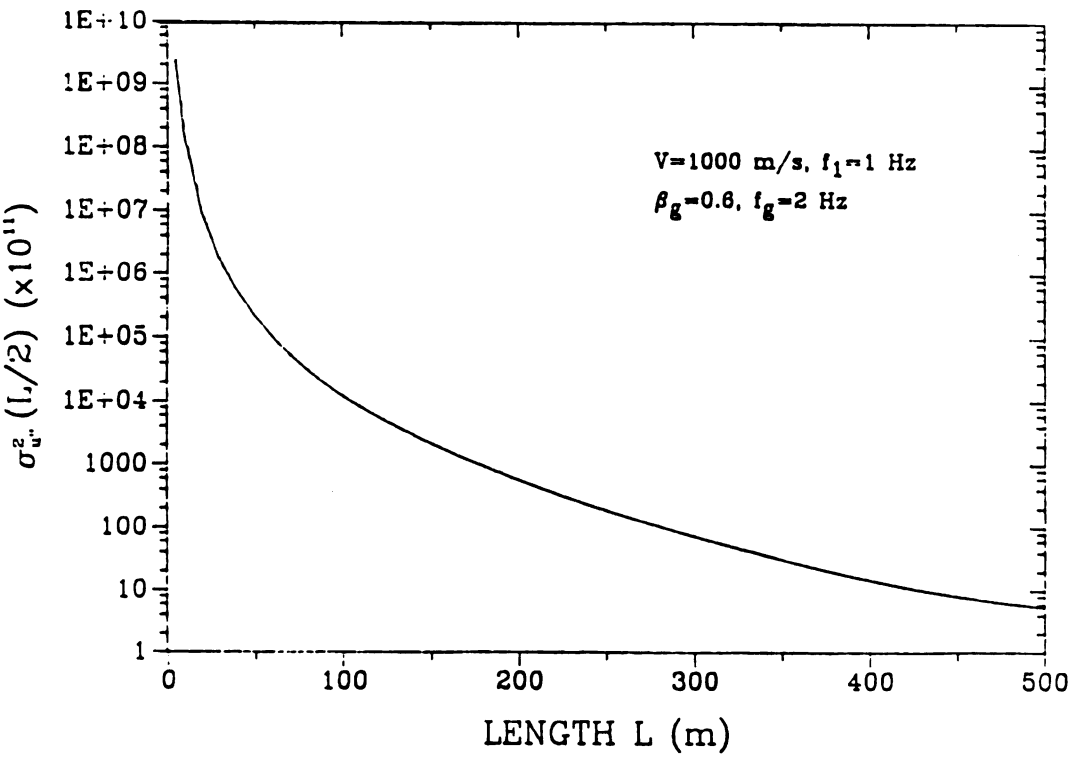

Figure 2-5 : Effect of Beam Length on $\sigma^2_{u''}$

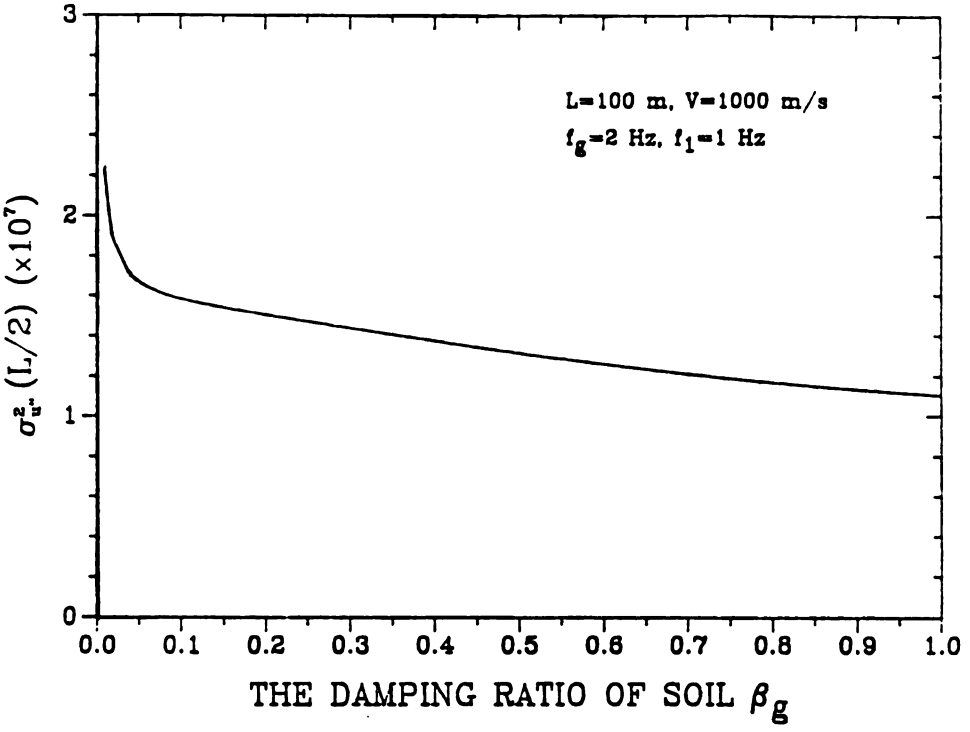

Figure 2-6 : Effect of β_g on $\sigma^2_{u''}$

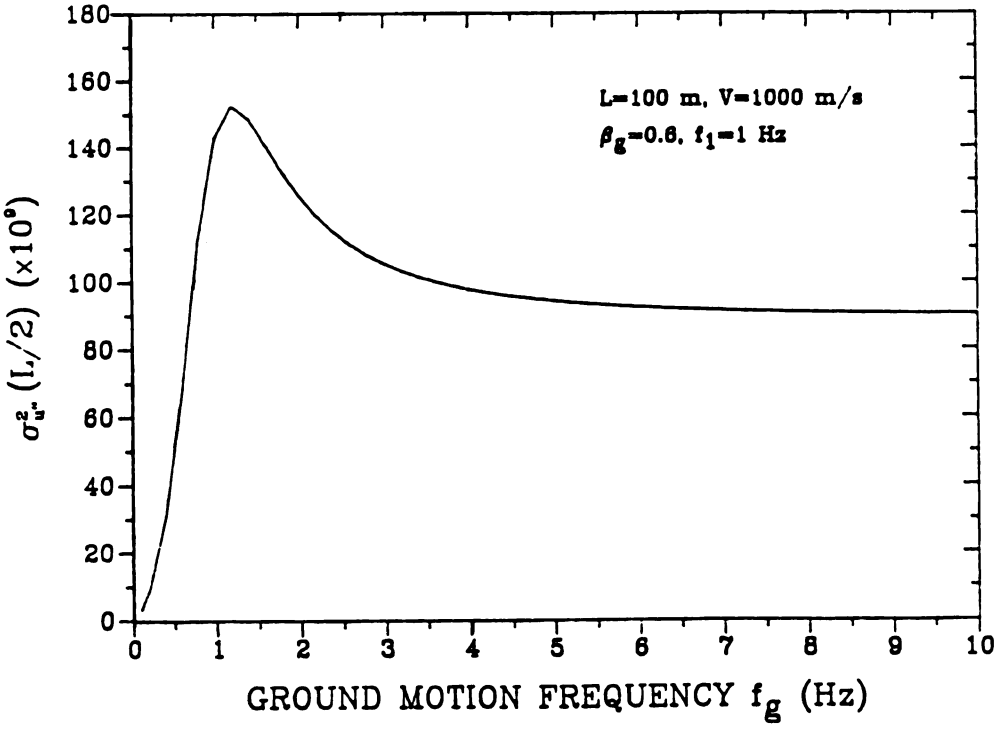

Figure 2-7 : Effect of Ground Motion Frequency on $\sigma^2_{u''}$

2.3.2 Some Special Cases

In order to examine the effect of correlation decay and phase shift between different support excitations on the response of the structure, we consider some special cases of support excitation.

Case 1: Fully correlated and in-phase excitations at supports A and B. This corresponds to the current practice of considering identical support excitations. For this case, $\rho \cos(\omega L/V) = 1$, and from equation (2-27) it is clear that only odd modes contribute to the response.

Case 2: Phase shift only. Here we assume that there is no loss in coherency between the support excitations at A and B, but that there is a time delay for seismic waves to propagate from A to B, i.e., $\rho = 1$.

Case 3: The excitations at supports A and B are uncorrelated, i.e., coherency is zero. For this case $\rho = 0$.

Case 4: No phase shift. If the waves propagate vertically, the excitations at every point would be in phase, i.e., there would be no time delay between support excitations at A and B and hence $\cos(\omega L/V) = 1$.

Case 5: Fully correlated but out-of-phase excitations at supports A and B. For this case $\rho \cos(\omega L/V) = -1$ and only the even modes contribute to the response.

Figures 2-8 to 2-15 show comparisons of the five special cases with the general case. In these figures, we denote the response variance for the general case by $\sigma^2_{u''}$ and those for case 1 to 5 by σ^2_i, $i = 1,2,\ldots5$. Since we are interested in the maximum response, for cases 1 to 4 the response ratio, $\sigma^2_i(L/2)/\sigma^2_{u''}(L/2)$, vs. the non-dimensionalized fundamental frequency of the beam, $f_1 L/V = \omega_1 L/(2\pi V)$, is plotted; for

case 5, the maximum values of variance are at quarter-span and three-quarter-span (the dominant mode being the second mode), and thus we consider the response ratio $\sigma_5^2(L/4)/\sigma_{u''}^2(L/2)$.

Figures 2-8 to 2-11 depict results for different lengths of the beam with V = 1000 m/s, β_g = 0.6 and f_g = 2 Hz. Figures 2-10 and 2-12 to 2-14 allow comparisons for various values of β_g and f_g with L = 100 m and V = 1000 m/s. From these results we can conclude that:

1) The longer the structure, the larger the relative difference between σ_i^2 and $\sigma_{u''}^2$. The maximum ratio of $\sigma_i^2/\sigma_{u''}^2$ increases from 1.5 to 4.5 as the length L increases from 20 m to 200 m. This clearly shows that the effect of spatial variation of ground motion on the response of the beam depends on the separation of the supports and the time delay for wave propagation.

2) The extremes of the ratio $\sigma_i^2/\sigma_{u''}^2$ occur at approximately $f_1 L/V = k/2$, $k = 1,2,3,\ldots$, for which $\cos(2\pi f_1 L/V) = -1$ and $+1$, i.e., when the excitations at frequency f_1 are predominantly out-of-phase and in-phase, respectively. At the minimum points, cases 1, 3 and 4 (which do not contain any phase shift) give higher responses than the general case (except for very short beams). Case 2 has a lower value of $\sigma_{u''}^2$ at the minimum points due to the assumption of fully out-of-phase excitations at all frequencies.

3) The variance of curvature for the fully correlated case is always higher than that for the general case. This is because there is no coherency loss between the support excitations for the fully correlated case. In equation (2-27), $\rho(L,f)$ represents the coherency between the two support excitations and it decreases very rapidly

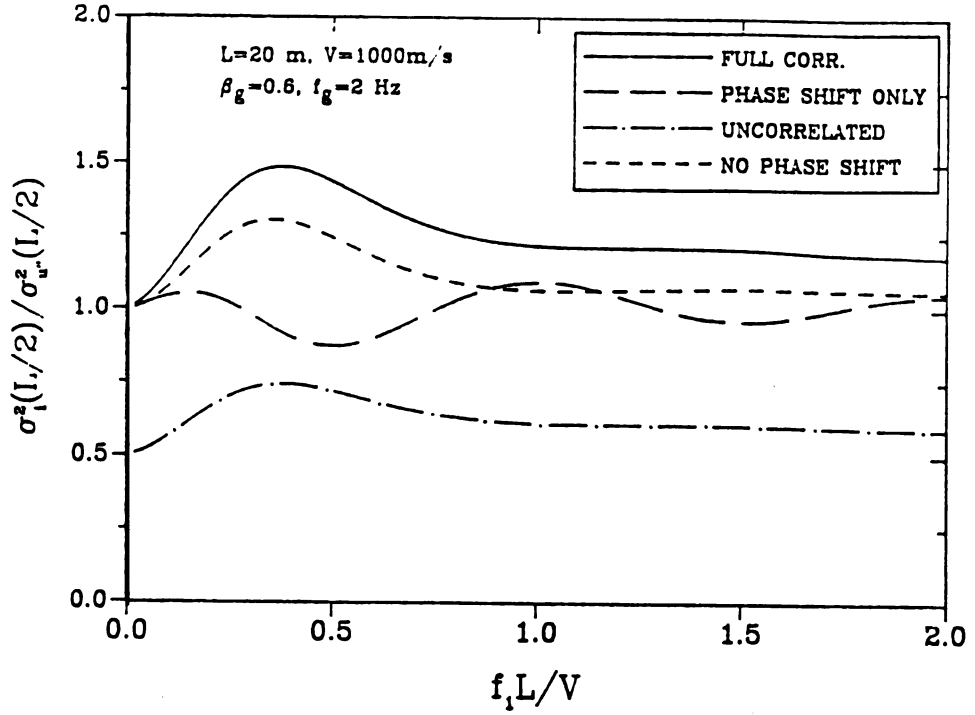

Figure 2-8 : Response Ratio for Cases 1 to 4 - L = 20 m

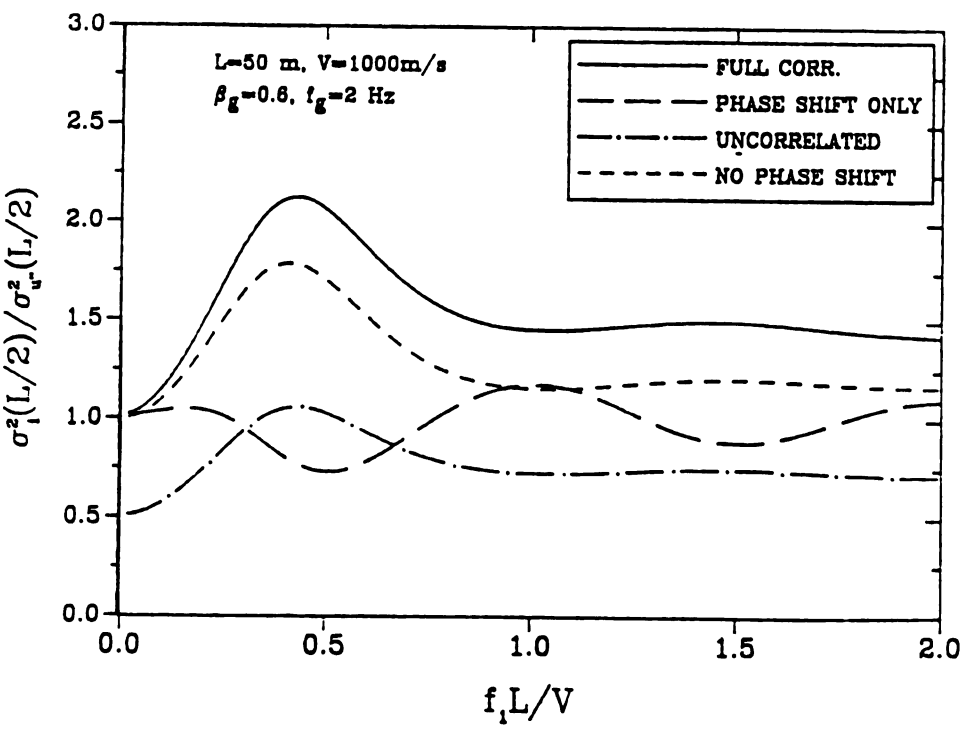

Figure 2-9 : Response Ratio for Cases 1 to 4 - L = 50 m

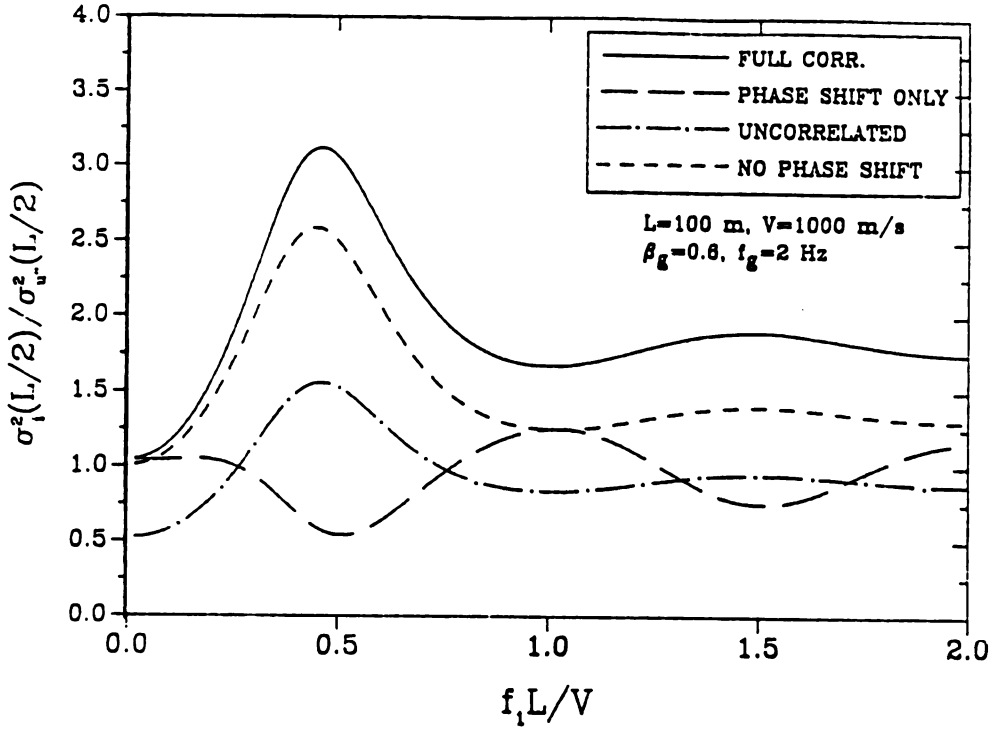

Figure 2-10: Response Ratio for Cases 1 to 4 - L = 100 m

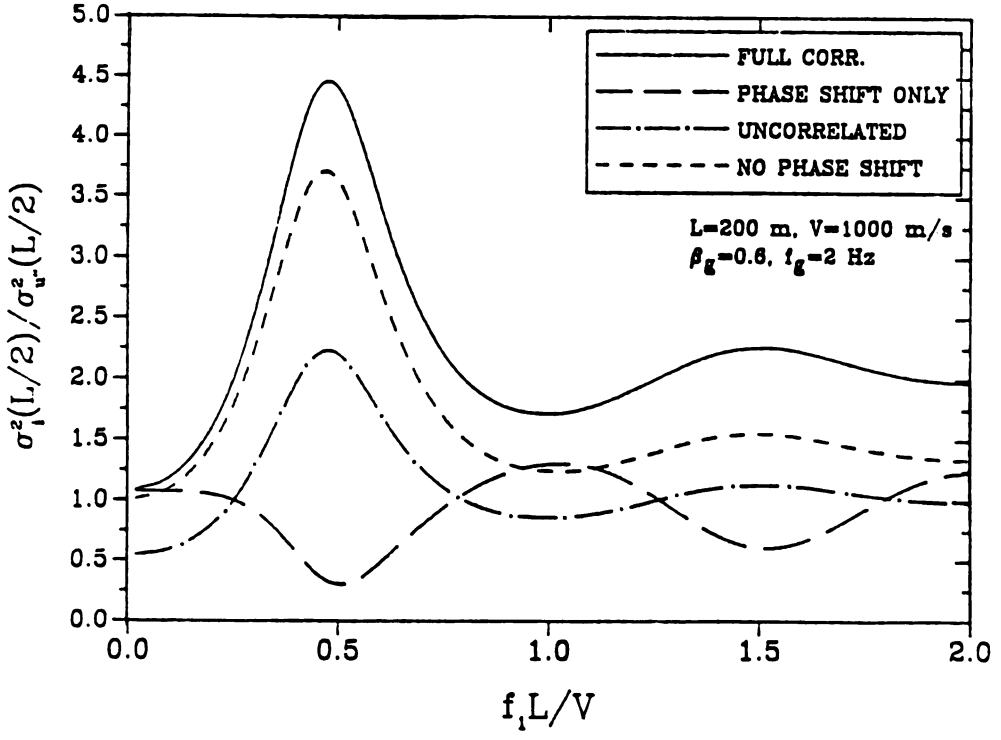

Figure 2-11: Response Ratio for Cases 1 to 4 - L = 200 m

with increasing L, and is close to zero for high natural requencies. On the other hand, the dominant contribution to the response comes from the first mode and when $\rho(L,f)$ is zero σ_1^2 will be equal to $2\sigma_{u''}^2$. This is why for longer beams (say, L > 200 m), $\sigma_1^2 \approx 2\sigma_{u''}^2$ for large f_1. The results also show that no matter how long the beam and how high the fundamental frequency, over-conservative estimates of the response are always obtained if fully correlated and in-phase excitations are assumed.

4) For case 5 (fully correlated but out-of-phase excitation), σ_5^2 is always much less than $\sigma_{u''}^2$ (see Figure 2-15). For this case, the first mode is not excited and hence the second mode is most dominant. Consequently the maximum value of σ_5^2 is at $f_1 \approx f_g/4$, i.e., $f_2 \approx f_g$. Note that the function $|H_j(\omega)|^2$ decreases very rapidly when ω_j increases ($\omega_j = j^2\omega_1$), and it is due to this that σ_5^2 is only 2 to 15 percent of the value of $\sigma_{u''}^2$.

5) For other cases, the response variances are sometimes over-predicted and sometimes under-predicted depending on the length L, fundamental frequency f_1 and wave velocity V. Here one point worth noting is that for case 4 (neglecting phase shift but considering coherency decay), the response is usually always higher than that for the general case. The difference, however, is relatively small ($\sigma_4^2/\sigma_{u''}^2$ usually being less than 1.5) when f_1L/V is greater than 1.

6) The values of f_g and β_g also have an effect on the ratio $\sigma_i^2/\sigma_{u''}^2$. From Figures 2-10 and 2-12 to 2-14 it is apparent that for the same length and velocity, the relative difference between σ_i^2 and $\sigma_{u''}^2$ becomes larger when f_g increases from 2 to 4 Hz. The ratio $\sigma_i^2/\sigma_{u''}^2$ also changes as β_g changes but no simple trend is apparent.

Of the five special cases, cases 1, 2, 3 and 5 do not consider the

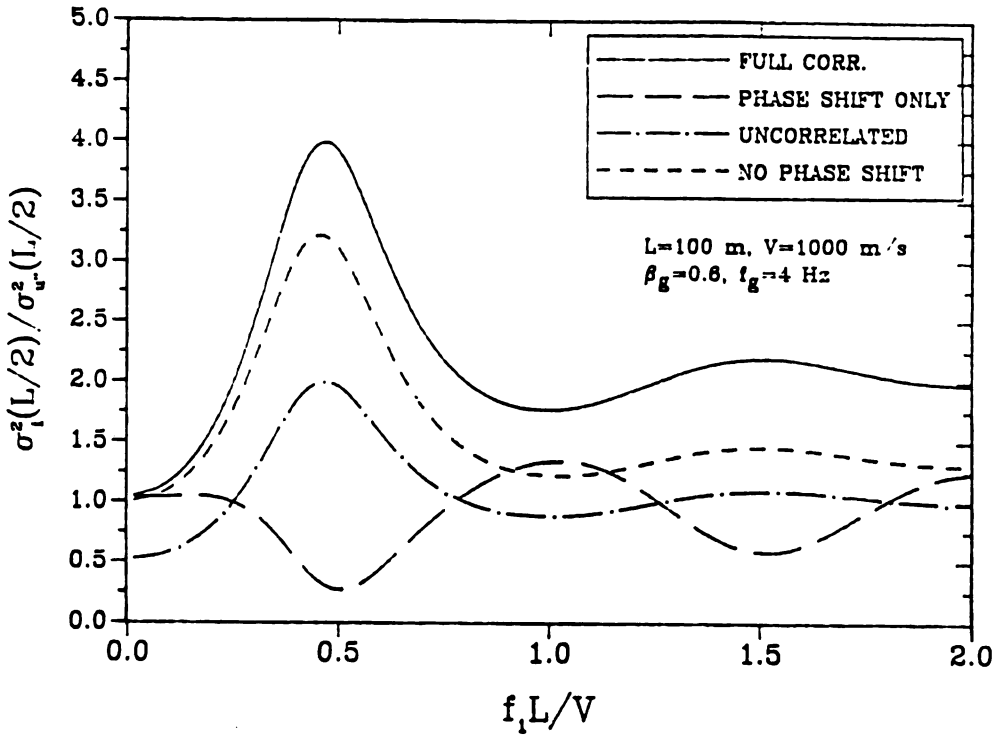

Figure 2-12: Response Ratio for Cases 1 to 4 - β_g = 0.6, f_g = 4 Hz

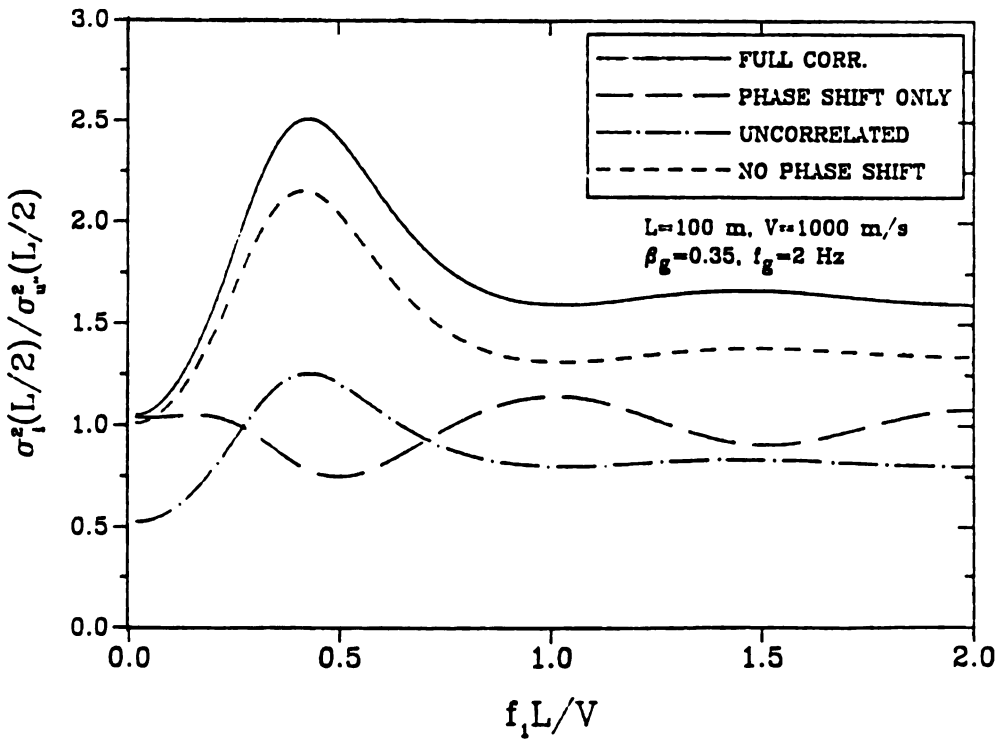

Figure 2-13: Response Ratio for Cases 1 to 4 - β_g = 0.35, f_g = 2 Hz

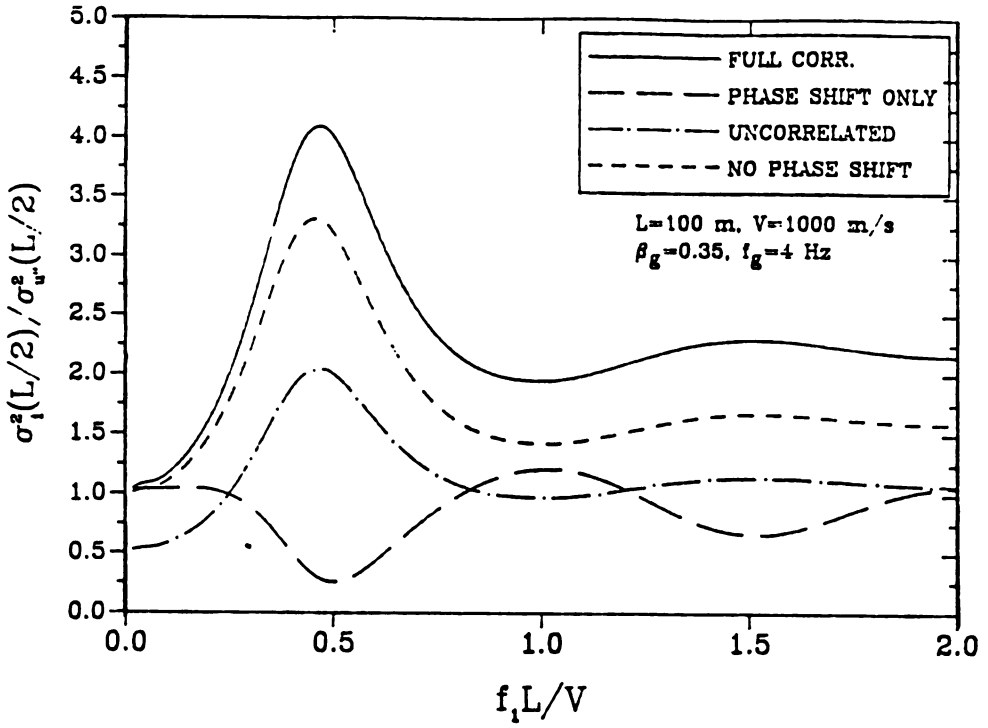

Figure 2-14: Response Ratio for Cases 1 to 4 - β_g = 0.35, f_g = 4 Hz

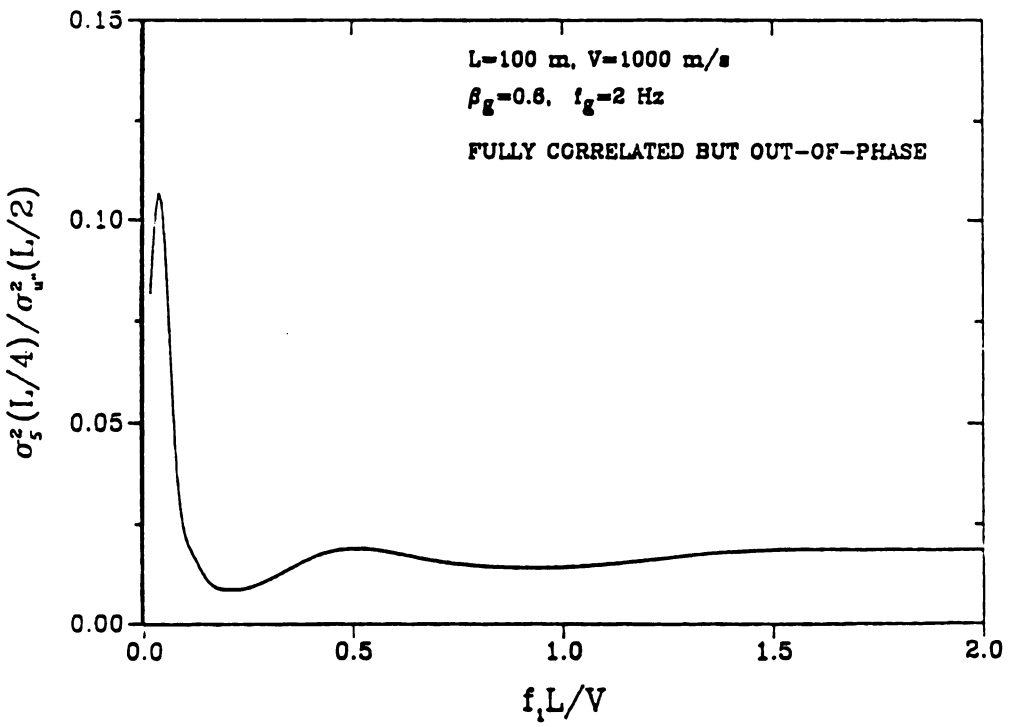

Figure 2-15: Typical Response Ratio for Case 5

correlation decay between different support excitations, so they are simpler than the general case; case 4 does not consider wave propagation but accounts for correlation decay. From the numerical results, it is apparent that the coherency affects the variance of curvature more than the time delay, and therefore in order to obtain more accurate response predictions, at least the correlation decay between difference support excitations should be taken into account.

2.4 Approximate Methods for Evaluating the Response Variance

Equation (2-27) allows the evaluation of the response variance of the beam excited by random ground motion. However, for practical purposes, it would be desirable to find an approximate method which simplifies the numerical computations while yielding reasonably accurate results.

Since the first mode response is most dominant, it should be easonable to consider only the first mode response in equation (2-27). i.e.,

$$\sigma^2_{u''}(x) \approx [\psi_1''(x)]^2 \int_{-\infty}^{\infty} |H_1(\omega)|^2 \, \Phi_{11}(\omega) \, d\omega \tag{2-29}$$

Assuming that $\Phi_{11}(\omega)$ is slowly varying in the vicinity of the narrow spike, $|H_1(\omega)|^2$, we obtain the commonly used approximation:

$$\int_{-\infty}^{\infty} \Phi_{11}(\omega) \, |H_1(\omega)|^2 \, d\omega \approx \Phi_{11}(\omega_1) \int_{-\infty}^{\infty} |H_1(\omega)|^2 \, d\omega$$

$$= \Phi_{11}(\omega_1) \, \frac{\pi}{2\zeta_1 \omega_1^3} \tag{2-30}$$

where the well-known result

$$\int_{-\infty}^{\infty} |H_1(\omega)|^2 \, d\omega = \frac{\pi}{2\zeta_1 \omega_1^3} \tag{2-31}$$

has been used. Thus we can write

$$\sigma^2_{u''}(x) \approx [\psi''_1(x)]^2 \, \Phi_{11}(\omega_1) \, \frac{\pi}{2\zeta_1 \omega_1^3} \tag{2-32}$$

The above approximation was evaluated for different beam lengths, and β_g and f_g values. Figures 2-16 and 2-17 give the percentage error of the approximation compared to exact value of $\sigma^2_{u''}$ at midspan. The results indicate that when the fundamental frequency of the beam, f_1, is small (say, lower then ground motion frequency f_g), the approximation is quite acceptable - the error usually being less than 10%. But when f_1 increases, the error also increases - up to -70% at f_1 = 10 Hz. In order to obtain better results, an improved approximation is necessary.

In order to derive an improved approximation, the behavior of the functions in equations (2-27) and (2-32) were investigated. Figures 2-18 and 2-19 show comparisons of the actual and approximate shapes of the product $\Phi_{11}(\omega)|H_1(\omega)|^2$. It can be seen that for f_1 = 1 Hz (i.e., $f_1 < f_g$), the actual curve and approximate curve almost coincide, but for f_1 = 5 Hz ($f_1 > f_g$) there is a significant deviation between the two curves. This is the main source of error. To reduce the error we can perhaps add a correction term when f_1 is large.

From the separate plots of $\Phi_{11}(\omega)$ and $|H_1(\omega)|^2$ plotted in Figures 2-20 and 2-21 it can be clearly seen that the maximum value of $\Phi_{11}(\omega)$ is at a frequency slightly lower than f_g, after which $\Phi_{11}(\omega)$ decays very quickly. For $|H_1(\omega)|^2$, the peak occurs approximately at $f = f_1$ and the values of $|H_1(\omega)|^2$ become very small when f departs from f_1. Note also that the magnitude of $|H_1(\omega)|^2$ decreases extremely rapidly at all frequencies when f_1 increases. Thus, when f_1 is larger than f_g, the product of $\Phi_{11}(\omega)$ and $|H_1(\omega)|^2$ becomes significant at the lower frequency range. We should, therefore, add a correction when f_1 is larger than

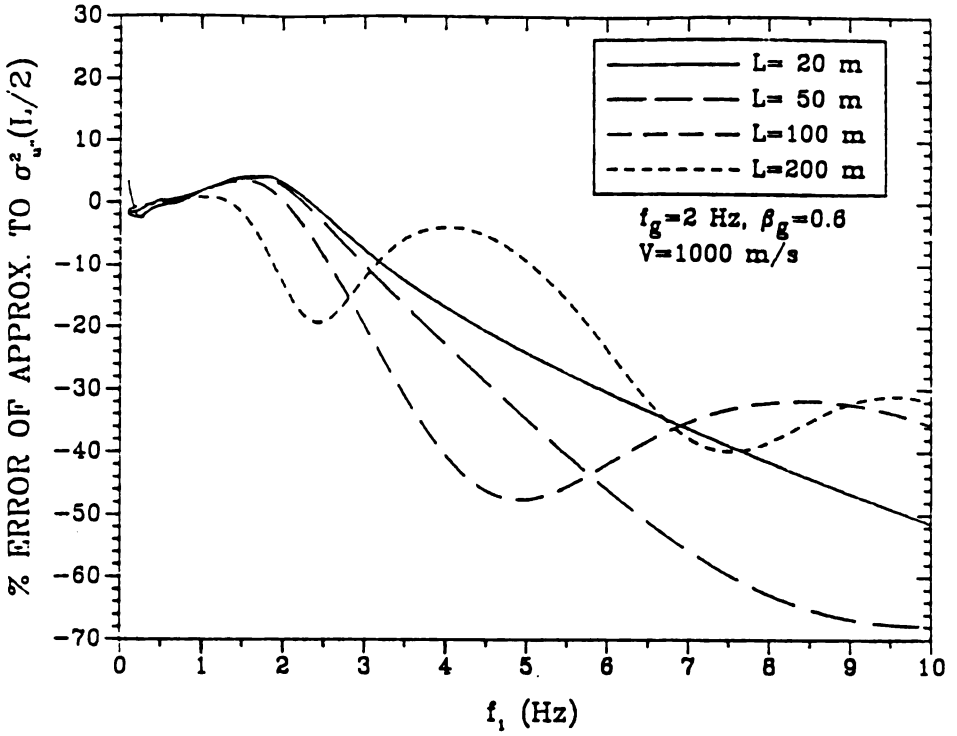

Figure 2-16: Errors of Approximation to $\sigma^2_{u''}$ for Different Beam Lengths

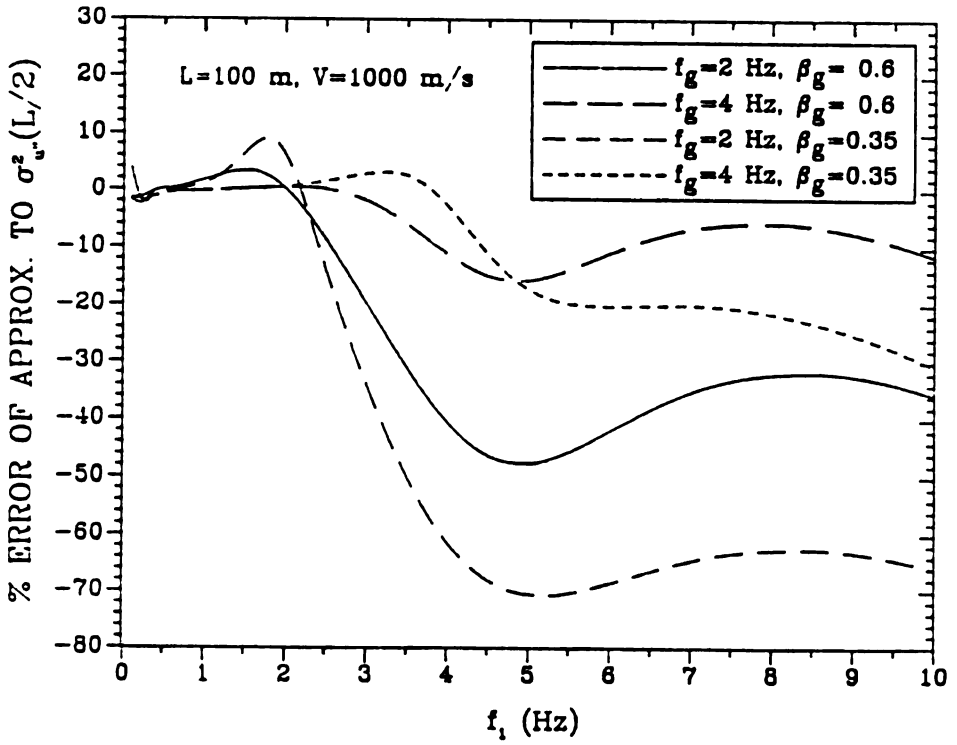

Figure 2-17: Errors of Approximation to $\sigma^2_{u''}$ for Different β_g and f_g

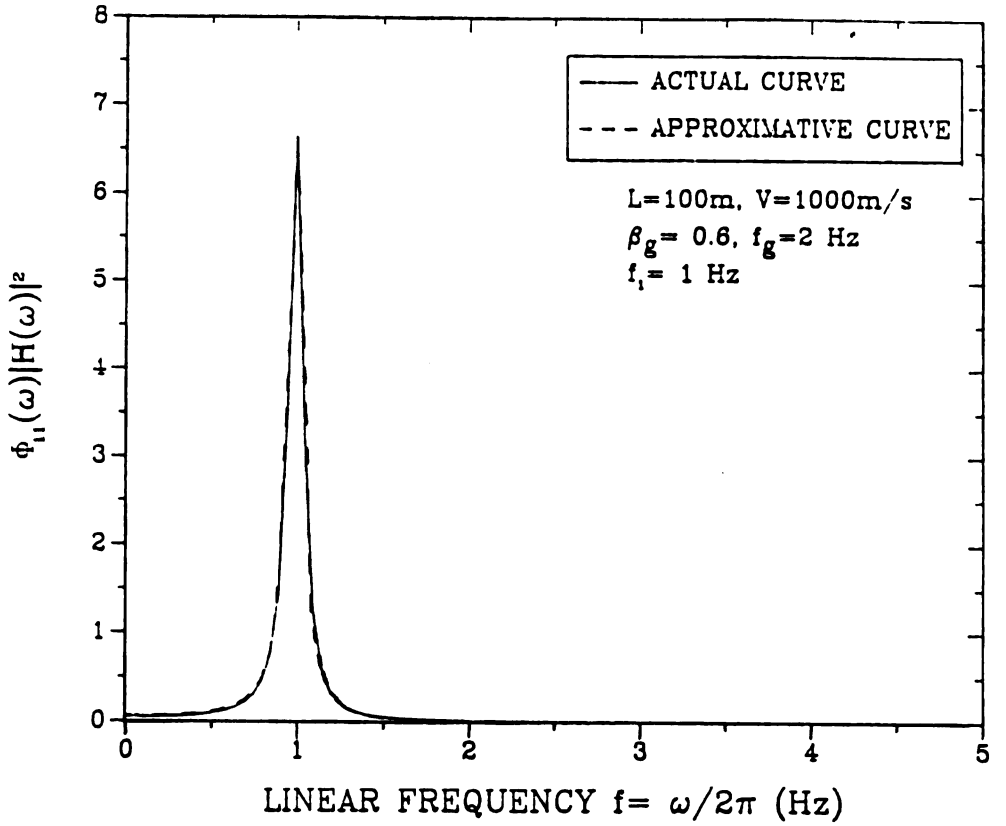

Figure 2-18: Plot of $\Phi_{11}(\omega)\ |H(\omega)|^2$ - L = 100 m, f_1 = 1 Hz

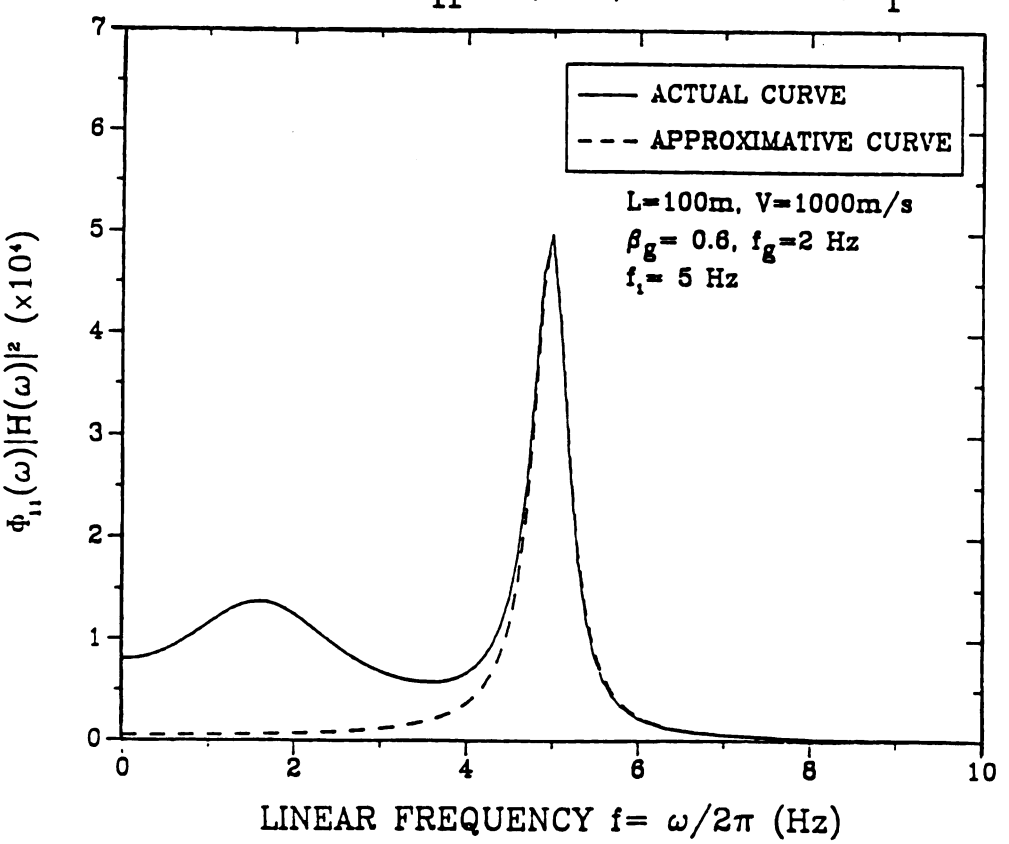

Figure 2-19: Plot of $\Phi_{11}(\omega)\ |H(\omega)|^2$ - L = 100 m, f_1 = 5 Hz

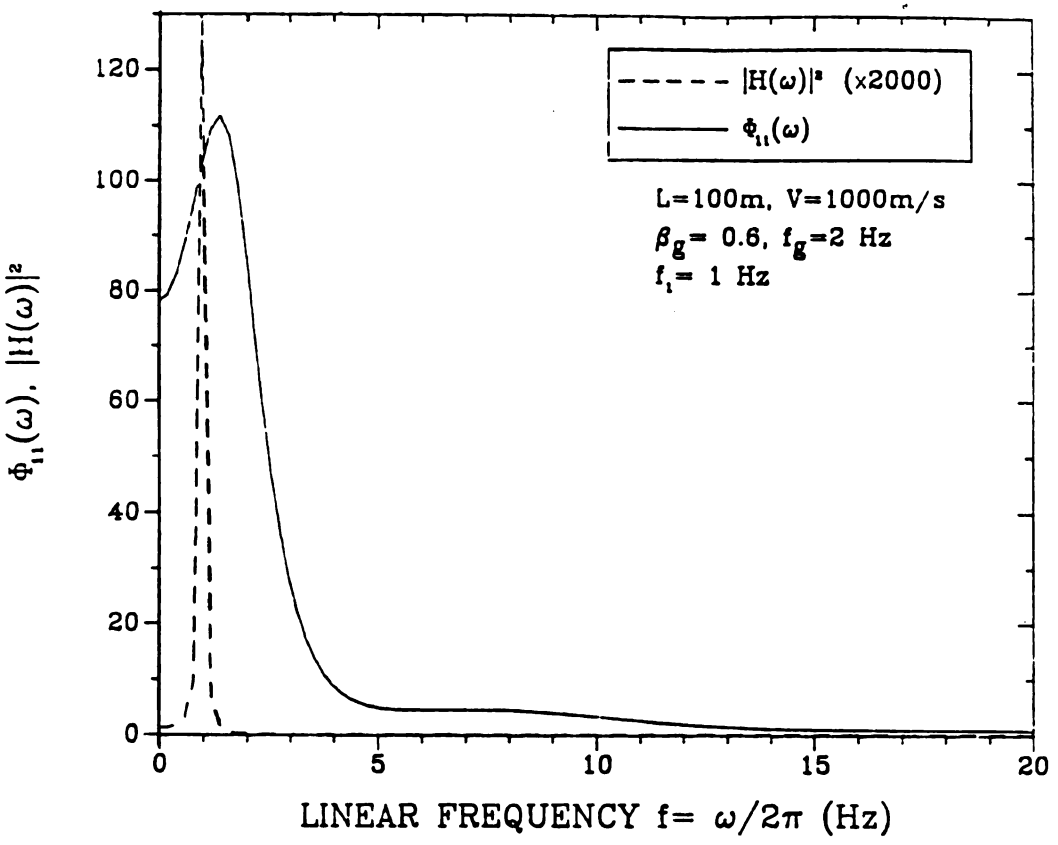

Figure 2-20: Plot of $\Phi_{11}(\omega)$ and $|H(\omega)|^2$ - L = 100 m, f_1 = 1 Hz

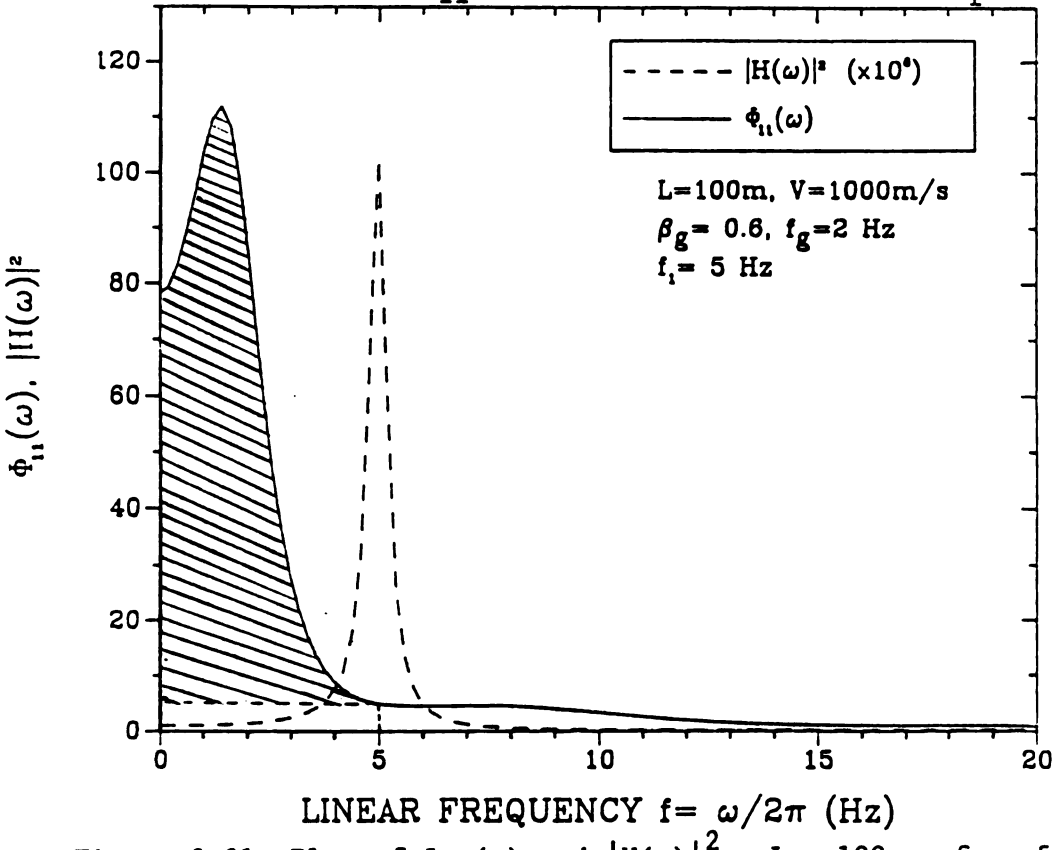

Figure 2-21: Plot of $\Phi_{11}(\omega)$ and $|H(\omega)|^2$ - L = 100 m, f_1 = 5 Hz

the frequency at which $\Phi_{11}(\omega)$ attains its maximum value.

To determine the frequency at which $\Phi_{11}(\omega)$ attains its maximum value is difficult for all conditions, but for the fully correlated case the peak occurs at the frequency at which the Kanai-Tajimi spectrum has its peak, namely

$$f_p = \left[\frac{(\sqrt{1 + 8\beta_g^2} - 1)^{1/2}}{2\beta_g}\right] f_g \qquad (2\text{-}33)$$

For small β_g, $f_p \approx f_g$. Figure 2-22 depicts plots of $\Phi_{11}(\omega)$ for different beam lengths and it shows that the location of the peak of $\Phi_{11}(\omega)$ changes for the general case depending on the parameters used. The frequency V/(4L) plays an important role, since cos (2πfL/V) becomes negative as f increases beyond V/(4L), and therefore $\Phi_{11}(\omega)$ begins to decrease (see equation (2-25)). If $f_p < V/(4L)$ then the peak of $\Phi_{11}(\omega)$ occurs near f_p, otherwise it occurs near V/(4L). Hence it would seem reasonable to add the correction when either f_1 is larger than f_p or V/(4L).

In equation (2-30) it was assumed that $\Phi_{11}(\omega)$ was constant and equal to $\Phi_{11}(\omega_1)$. The shaded area of $\Phi_{11}(\omega)$ shown in Figure 2-21 was not accounted for. Assuming that in the frequency range from 0 to $\omega_1 = 2\pi f_1$ we can approximate $|H_1(\omega)|^2$ by $|H_1(0)|^2 = 1/\omega^4$, the correction to equation (2-31) may be written as

$$\Delta\sigma^2(x) = \frac{1}{\omega^4}\,[\psi_1''(x)]^2 \times (\text{shaded area in Figure 2-21})$$

$$= \frac{1}{\omega^4}\,[\psi_1''(x)]^2 \left[\int_0^{\omega_1} \Phi_{11}(\omega)\,d\omega - \omega_1 \Phi_{11}(\omega_1)\right] \qquad (2\text{-}34)$$

The integral in the above equation may be evaluated through a numerical quadrature rule such as Simpson's rule. The integrand is now

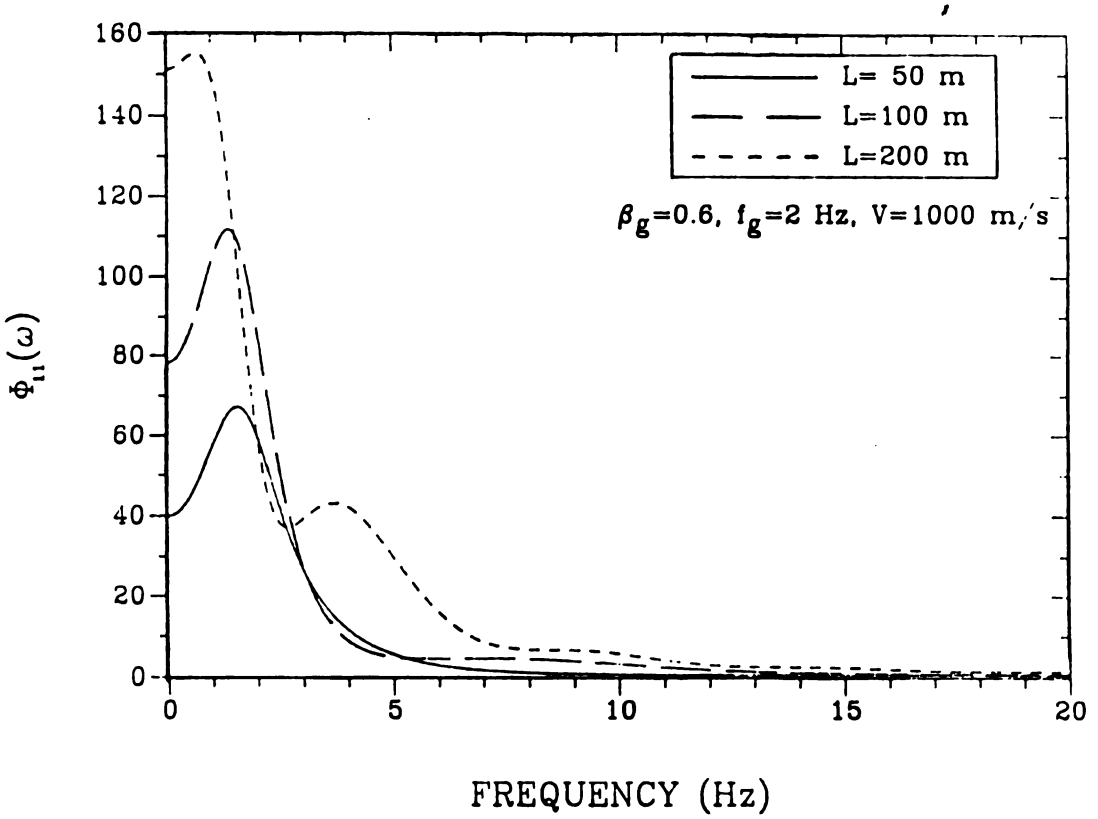

Figure 2-22: Plot of $\Phi_{11}(\omega)$ for Different Beam Lengths

a smoothly varying function without the peak-like behavior of $|H_1(\omega)|^2$ and can therefore be evaluated easily without significant error.

The corrected approximation may thus be summarized as follows:

$$\sigma^2_{u''}(x) = \begin{cases} [\psi_1''(x)]^2 \Phi_{11}(\omega_1) \frac{\pi}{2\beta_1 \omega_1^3} , & \text{when } \omega_1 \le \omega_p \text{ and } \omega_1 \le \frac{\pi V}{2L} \\ [\psi_1''(x)]^2 \Phi_{11}(\omega_1) \frac{\pi}{2\beta_1 \omega_1^3} + \Delta\sigma^2_{u''} , & \text{elsewhere} \end{cases} \quad (2\text{-}35)$$

where $\omega_p = 2\pi f_p$.

Figures 2-23 and 2-24 show the percentage errors between the corrected approximation and the exact solution of $\sigma^2_{u''}$ at midspan. As expected, the errors are greatly reduced. The corrected approximation was usually accurate to within 15%, although for some cases it was in error by about 25%. In all cases the corrections substantially improved

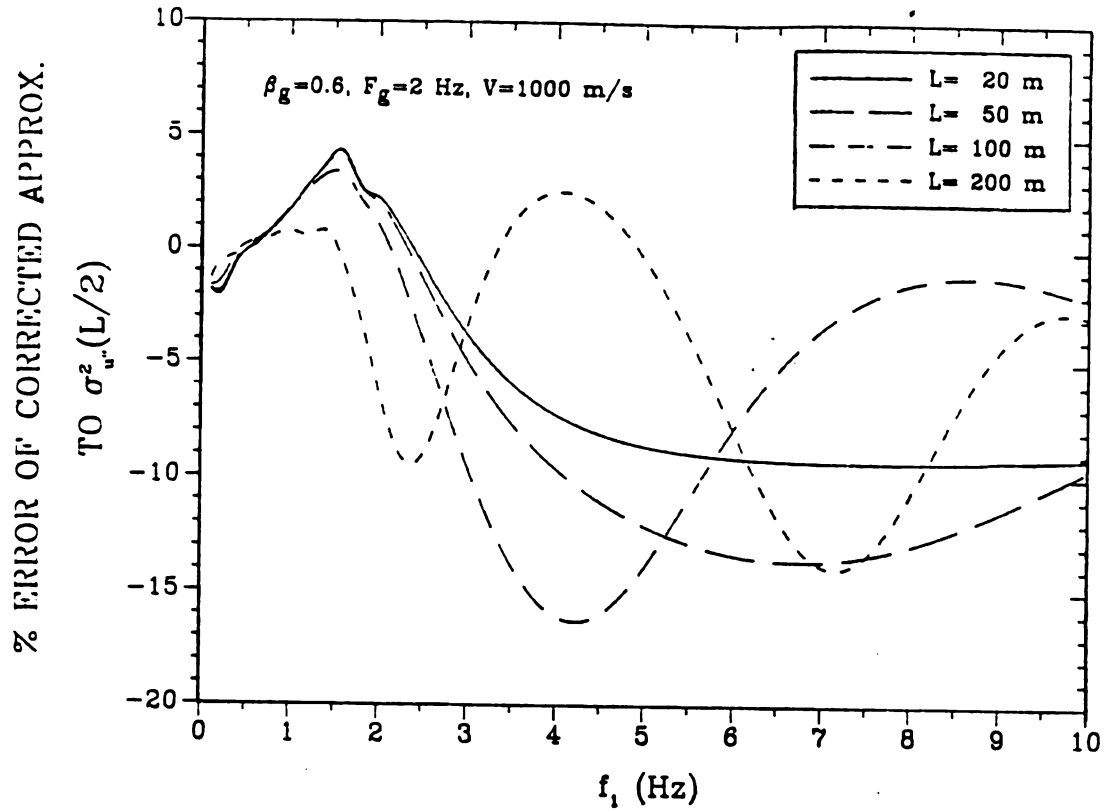

Figure 2-23: Errors of Corrected Approx. to $\sigma^2_{u''}$ for Various Beam Lengths

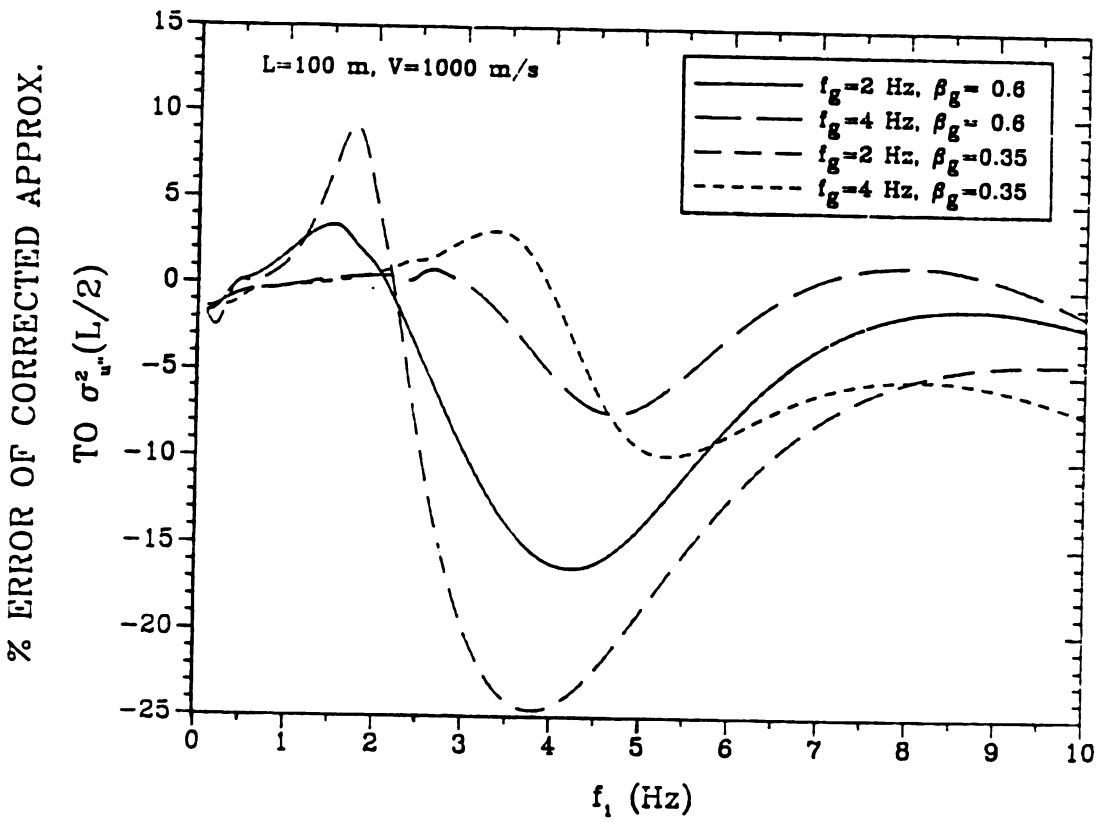

Figure 2-24: Errors of Corrected Approx. to $\sigma^2_{u''}$ for Various β_g and f_g

the variance estimates.

Finally, the distribution along the length of the beam of the exact solution, the exact first mode reponse, and the corrected approximation, are compared in figures 2-25 to 2-28. The variance $\sigma^2_{u''}(x)$ is normalized by $\sigma^2_{u'',exact}(L/2)$ in these firgures, and it can be seen that the corrected approximation matches the exact first mode solution very well. As discussed earlier, for some cases there are errors arising from considering only the first mode, especially when $f_1 = f_g/4$ (for which case the second mode response gives significant contribution). But as far as the maximum responses are concerned the approximation is still acceptable.

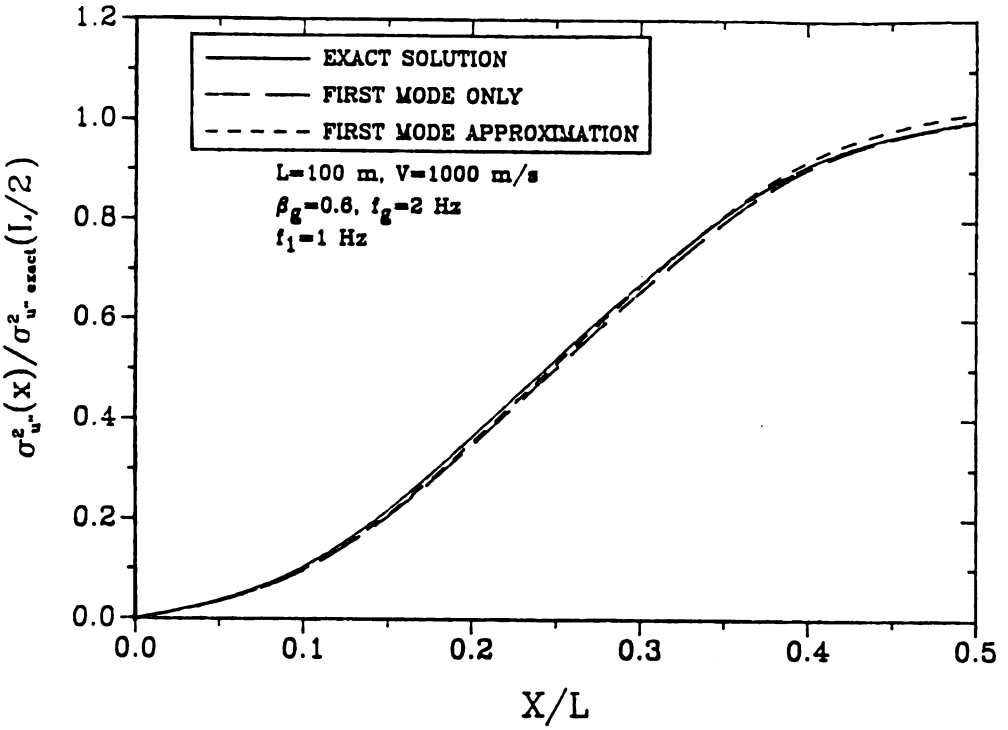

Figure 2-25: Variation of $\sigma^2_{u''}$ Along the Length - β_g = 0.6, f_g = 2 Hz

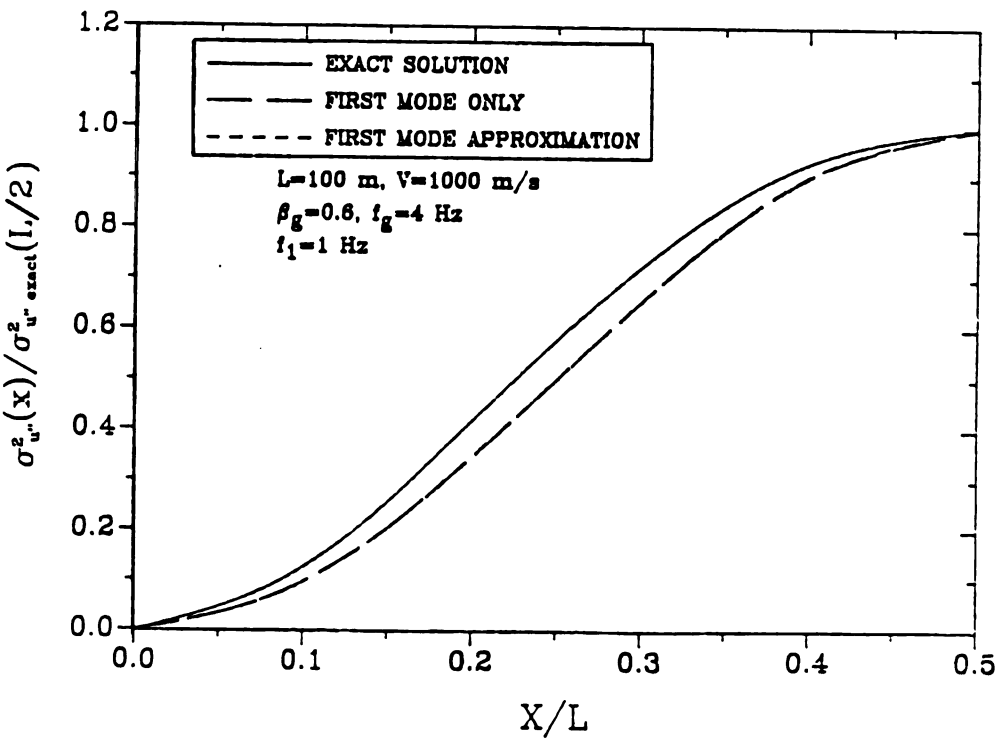

Figure 2-26: Variation of $\sigma^2_{u''}$ Along the Length - β_g = 0.6, f_g = 4 Hz

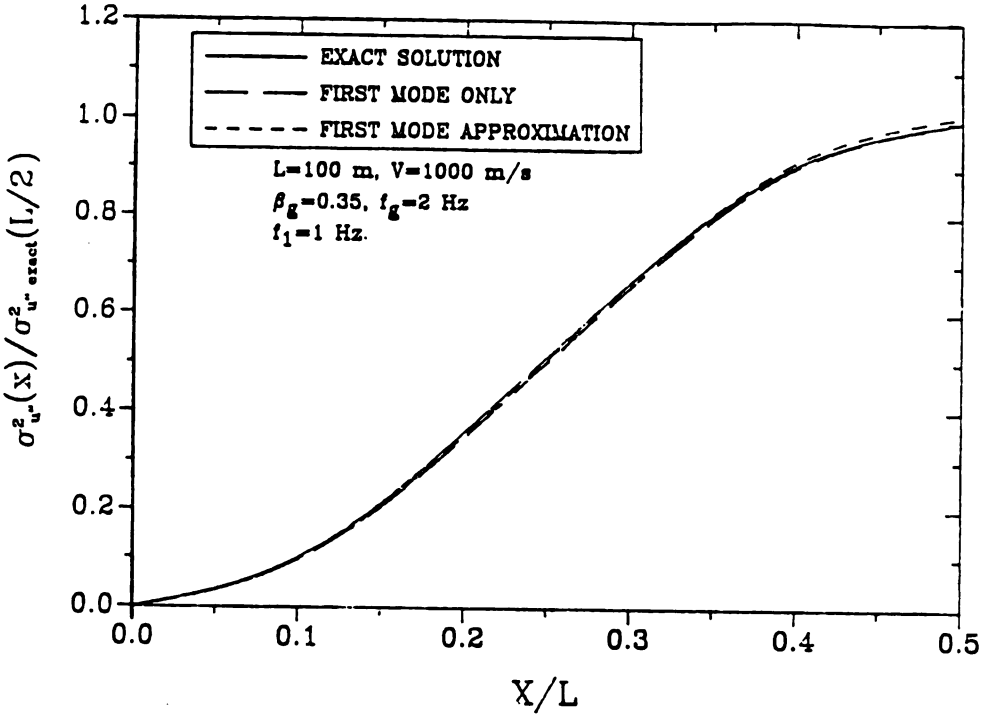

Figure 2-27: Variation of $\sigma^2_{u''}$ Along the Length - β_g = 0.35, f_g = 2 Hz

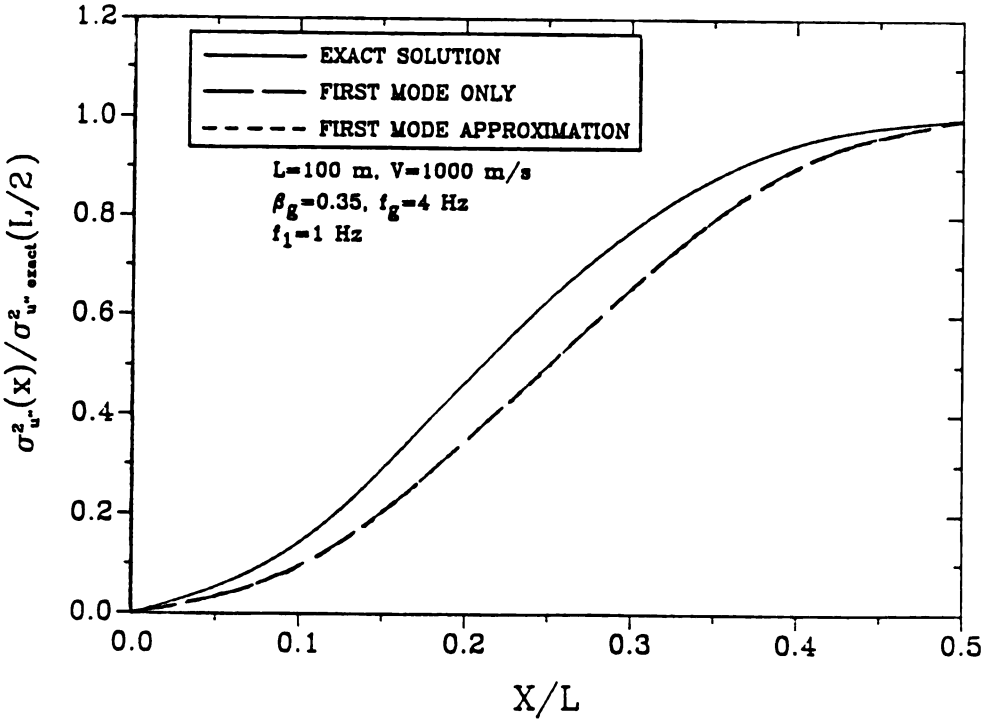

Figure 2-28: Variation of $\sigma^2_{u''}$ Along the Length - β_g = 0.35, f_g = 4 Hz

3. CONCLUSIONS

From the above study of the response of a simply supported beam to differential support excitations caused by the spatial variation of ground motion, the following conclusions may be drawn:

1) The spatial variation of ground motion will significantly affect the response of structures to the random ground motion, especially for long structures;

2) The excitation condition (or input condition) is very important for estimating the response of structures to ground motion. For simply-supported beam-like structures, assuming identical support excitations will lead to conservative response estimates compared to the general case which includes correlation decay and phase delay. Assuming out-of-phase fully correlated support excitation is un-reasonable and will seriously under-predict the responses.

3) The correlation between support excitations is more important than the time delay (or phase shift) in predicting the response for typical simply-supported bridge lengths and seismic wave velocities.

4) The response of a beam-like structure to random ground motion is very sensitive to the length and the fundamental frequency of the structure, though the properties of the ground soil also affect the response.

5) For a simply supported beam, estimates of the response to correlated support excitations obtained by considering only the fundamental

modal response yields sufficiently accurate results. For practical purposes, the proposed approximate method can be used to obtain very reasonable results with a minimum of computations. If the natural frequency of the structure is very low (lower than one quarter of the ground motion frequency), consideration of higher mode responses will give better results, since higher mode frequencies may lie within the dominant excitation frequency range.

LIST OF REFERENCES

LIST OF REFERENCES

1. Bolt, B.A., Abrahamson, N., and Yeh, Y.T. (1984). "The Variation of Strong Ground Motion Over Short Distances," *Proceedings of the Eighth World Conference on Earthquake Engineering*, 183-189.

2. Crandall, S.H. (1979). "Random Vibration of One- and Two-Dimensional Structures," in *Developments in Statistics*, P.R. Krishnaiah (ed), Academic Press.

3. Harichandran, R.S., and Vanmarcke, E. (1986). "Stochastic Variation of Earthquake Ground Motion in Space and Time," *Journal of Engineering Mechanics*, ASCE, 112(2), 154-174.

4. Harichandran, R.S. (1987). "Stochastic Analysis of Rigid Foundation Filtering," *Earthquake Engineering and Structural Dynamics*, 15(7), 889-899.

5. Loh, C-H., Penzien, J., and Ysai, Y.B. (1982). "Engineering Analysis of SMART 1 Array Accelerograms," *Earthquake Engineering and Structural Dynamics*, 10, 575-591.

6. Masri, S.F. (1976). "Response of Beams to Propagating Boundary Excitation," *Earthquake Engineering and Structural Dynamics*, 4, 497-507.

7. Masri, S.F. and Udwadia, F.E. (1977). "Transient Response of a Shear Beam to Correlated Random Boundary Excitation," *Journal of Applied Mechanics*, Transactions of the ASME, 44(E3), 487-491.

8. Scanlan, R.H. (1976). "Seismic Wave Effects on Soil-Structure Interaction," *Earthquake Engineering and Structural Dynamics*, 4, 379-388.

9. Vanmarcke, E. (1976). "Structural Response to Earthquakes," in *Seismic Risk and Engineering Decisions*, E. Rosenblueth and C. Lomnitz (editors), Elsevier, Amsterdam, 287-337.